UNIDIRECTIONAL YAGI-UDA ANTENNA DESIGN FOR 4G LTE COVERAGE ENHANCEMENT

'AIN SABRINA BINTI HAIROL ASHAR

UNIVERSITI TEKNIKAL MALAYSIA MELAKA

UNIDIRECTIONAL YAGI-UDA ANTENNA DESIGN FOR 4G LTE COVERAGE ENHANCEMENT

'AIN SABRINA BINTI HAIROL ASHAR

This report is submitted in partial fulfilment of the requirements for the degree of Bachelor of Electronic Engineering with Honours

Faculty of Electronic and Computer Technology and Engineering Universiti Teknikal Malaysia Melaka

2024

UNIVERSITI TEKNIKAL MALAYSIA MELAKA
FAKULTI TEKNOLOGI DAN KEJUTERAAN ELEKTRONIK DAN KOMPUTER

BORANG PENGESAHAN STATUS LAPORAN
PROJEK SARJANA MUDA II

Tajuk Projek   :   Unidirectional Yagi-Uda Antenna Design for 4G LTE Coverage Enhancement

Sesi Pengajian   :   2022/2023

Saya 'AIN SABRINA BINTI HAIROL ASHAR mengaku membenarkan laporan Projek Sarjana Muda ini disimpan di Perpustakaan dengan syarat-syarat kegunaan seperti berikut:

1. Laporan adalah hakmilik Universiti Teknikal Malaysia Melaka.
2. Perpustakaan dibenarkan membuat salinan untuk tujuan pengajian sahaja.
3. Perpustakaan dibenarkan membuat salinan laporan ini sebagai bahan pertukaran antara institusi pengajian tinggi.
4. Sila tandakan (✓):

☐ **SULIT***   (Mengandungi maklumat yang berdarjah keselamatan atau kepentingan Malaysia seperti yang termaktub di dalam AKTA RAHSIA RASMI 1972)

☐ **TERHAD***   (Mengandungi maklumat terhad yang telah ditentukan oleh organisasi/badan di mana penyelidikan dijalankan.

☑ **TIDAK TERHAD**

Disahkan oleh:

_____
(TANDATANGAN PENULIS)

_____
(COP DAN TANDATANGAN PENYELIA)

Alamat Tetap: No.18 Jalan 2/2A Seksyen 2, Bnadar Rinching 43500 Semenyih, Selangor

DR. IMRAN BIN MOHD IBRAHIM
Associate Professor
Faculty of Electronic and Computer Engineering
Universiti Teknikal Malaysia Melaka (UTeM)
Hang Tuah Jaya
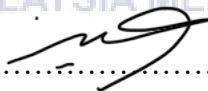76100 Durian Tunggal, Melaka

Tarikh :   24 Januari 2024

Tarikh : 24 Januari 2024

DECLARATION

I declare that this report entitled "Unidirectional Yagi-Uda Antenna Design for 4G LTE Coverage Enhancement" is the result of my own work except for quotes as cited in the references.
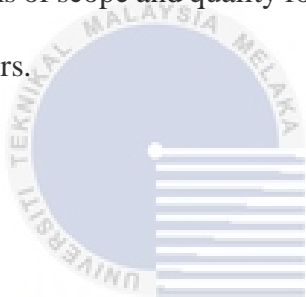
Signature : …………………………………….

Author : 'Ain Sabrina binti Hairol Ashar

Date : 24th January 2024

APPROVAL

I hereby declare that I have read this thesis and in my opinion this thesis is sufficient in terms of scope and quality for the award of Bachelor of Electronic Engineering with Honours.

Signature : ....

Supervisor Name : Profesor Madya Dr. Imran bin Mohd Ibrahim

Date : 24th January 2024

DEDICATION

I dedicate this thesis to all of the people who have contributed significantly to my academic career by providing constant encouragement, guidance, and support

Dedication to Profesor Madya Dr. Imran bin Mohd Ibrahim for his great guidance and support. Your astute criticism has been crucial in guiding me throughout the journey of completing the final year project.

To my family, the foundation of my success has always been their everlasting love and faith in my abilities. Your unflinching support is demonstrated by this thesis.

To my friends, whose unflagging encouragement, comradery, and sporadic diversion have given me the much-needed balance.

ABSTRACT

This project aims to develop a 4G antenna for enhancing 4G LTE coverage in a specific area. The chosen antenna is a rectangular-disk Yagi antenna, and the analysis of its radiation pattern and return-loss gain revealed that the maximum gain is achieved at the antenna's operating frequency in Band 7 of the 4G LTE spectrum. To enhance performance, an array technique was employed, involving a reduction in the width of the antenna elements. Initially, simulated results for return loss and gain were not obtained at the desired frequency of 2.6GHz but were achieved at 2.3GHz, showing values of -13.44dB and 4.28dBi, respectively. However, through the optimization of element width, the antenna successfully responded at 2.6GHz, resulting in a significant improvement from -13.44dB to -15.02dB for return loss, from 4.28dBi to 11.74dBi for gain and 94.51% efficiency. Additional 4G LTE band was acquired at 2.3GHz in Band 40 with return loss of -30.14dB, 12.07dBi gain and 99.31% efficiency. Subsequently, a model was fabricated and tested to validate the antenna design, and the measured results aligned well with the simulated ones. In conclusion, the project effectively enhances internet connection quality when the antenna is present, marking its completion and successful achievement of objectives.

ABSTRAK

Projek ini bertujuan untuk membangunkan antenna 4G bagi meningkatkan liputan 4G LTE di kawasan tertentu. Antenna yang dipilih adalah antenna Yagi berbentuk cakera segi empat, dan analisis corak radiasinya dan keuntungan kerugian pulangan menunjukkan bahawa keuntungan maksimum dicapai pada frekuensi operasi antenna dalam Jalur 7 spektrum 4G LTE. Bagi meningkatkan prestasi, teknik larik digunakan, melibatkan pengurangan lebar elemen antenna. Pada awalnya, hasil simulasi untuk keuntungan pulangan dan keuntungan tidak diperoleh pada frekuensi yang diinginkan iaitu 2.6GHz tetapi berjaya pada 2.3GHz, dengan nilai -13.44dB dan 4.28dBi masing-masing. Walau bagaimanapun, melalui optimasi lebar elemen, antenna berjaya memberi respons pada 2.6GHz, menghasilkan peningkatan yang signifikan dari -13.44dB kepada -15.02dB untuk keuntungan pulangan, dari 4.28dBi kepada 11.74dBi untuk keuntungan, dan 94.51% kecekapan. Jalur 4G LTE tambahan diperoleh pada 2.3GHz di Jalur 40 dengan keuntungan pulangan -30.14dB, keuntungan 12.07dBi, dan kecekapan 99.31%. Seterusnya, model ini difabrikasi dan diuji untuk mengesahkan reka bentuk antenna, dan hasil pengukuran sejajar dengan simulasi. Kesimpulannya, projek ini berkesan meningkatkan kualiti sambungan internet apabila antenna berada, menandakan penyelesaian dan pencapaian matlamat yang berjaya.

ACKNOWLEDGEMENTS

I would like to convey my sincerest gratitude to The Almighty and everyone who believed in and helped me finish this project. I would especially want to thank Prof esorMadya Dr Imran bin Mohd Ibrahim, who served as my project supervisor and who encouraged and advised us throughout the project's completion process. Additionally, he contributed to the project's organization, particularly throughout the writing of this report.

Additionally, I would like to express my gratitude to the Faculty of Electronic and Computer Engineering for providing me with the financing necessary to complete my final year project at University Technical Malaysia Melaka. I would like to extend my gratitude to the technicians of the PSM & Fabrication Lab and Research Lab, particularly Mr. Suffian and Mr. Imran, for providing the equipment and guidance throughout the journey of completing this project.

Finally, I would like to extend my sincere gratitude to my most beloved parents for their unfailing love, support, and compassion.

TABLE OF CONTENTS

LIST OF FIGURES

LIST OF TABLES

LIST OF SYMBOLS AND ABBREVIATIONS

IEEE   :   Institute of Electrical and Electronics Engineers

Wi-Fi   :   Wireless Fidelity

4G   :   4th Generation

LTE   :   Long-Term Evolution

MHz   :   Mega Hertz

CST   :   Computer Simulation Technology

ISP   :   Internet Service Provider

DSL   :   Digital Subscriber Line

LAN   :   Local Area Network

Mbps   :   Megabits per second

MAN   :   Metropolitan Area Network

VHF   :   Very High Frequency

UHF   :   Ultrahigh Frequency

dB   :   Decibels

GHz   :   Giga Hertz

HPBW   :   Half Power Beam Width

3D	:	3 Dimension
EM	:	Electromagnetic
SMA	:	Subminiature Version A
2D	:	2 Dimension
LMR240	:	Last-Minute Resistance
RSSI	:	Received Signal Strength Indicator
RF		Radio Frequency
RSRP		Reference Signal Received Power
RSRQ		Reference Signal Received Quality
SINR		Signal-to-interference-plus-noise ratio

LIST OF APPENDICES

CHAPTER 1

INTRODUCTION

1.1 Project Background

LTE, or long-term evolution, stands as a fourth generation (4G) wireless standard that offers improved network capacity and speed for mobile devices compared to its predecessor, third-generation technology. In today's world, LTE has become indispensable, especially after the emergence of Covid-19, leading to increased internet usage across various industries such as education, business, and Industry 4.0. Despite this surge in demand, certain areas still face challenges in accessing a reliable internet connection. The root cause often lies in the lack of infrastructure, particularly in regions where the cell towers are situated far from residential areas. To address these connectivity issues, there is a need for an antenna with specific characteristics, including high directivity, return loss lower than -10dB, and substantial gain. This project focuses on designing such an antenna to enhance 4G LTE coverage in areas

with poor internet connections, specifically targeting the 2.6GHz frequency band. The design process involves utilizing CST Software for antenna design, analyzing element widths, and optimizing the antenna to achieve favorable outcomes in terms of return loss, directivity, efficiency, and gain. The ultimate goal of this project is to develop a Yagi-Uda antenna that can effectively enhance 4G LTE coverage. This improved antenna is anticipated to contribute to the community by providing a reliable and robust internet connection, addressing the challenges faced in areas with subpar connectivity.

1.2   Problem Statement

In the wake of the Covid-19 pandemic, internet connectivity has become an essential requirement across all age groups. Its widespread use in education, business, healthcare, and daily activities highlights its pivotal role as a communication tool. Telecommunication companies have facilitated internet access at residences, business establishments, and workplaces to meet the escalating demand. Despite this vital role, some areas, particularly rural regions, continue to grapple with inadequate internet connectivity.

Challenges in rural areas arise from signal attenuation caused by surface obstacles, buildings, and varied geographical terrains. This issue severely impacts the transmission signal strength, particularly in mobile applications essential for daily functions in schools, offices, and mosques. Establishing reliable high-speed internet in rural locales proves more challenging than in urban centers due to the often-limited infrastructure for fiber optic connections. Although governments emphasize the need to bring high-speed internet to rural areas, practical implementation is hindered by the

cost-effectiveness of fiber optics, requiring subsidies for Internet Service Providers (ISPs).

Despite increased funding for rural broadband, these communities often rely on cable, digital subscriber line (DSL), satellite, hotspot, hybrid fiber-coaxial, or fiber connections [1]. The drawback lies in the fact that many of these lines cater to a small consumer base, leading to slower telecommunications company maintenance and repair times. Consequently, the prospect of upgrading to advanced quality standards remains uncertain.

1.3   Project Objective

The objectives of the projects are stated as follows:

I.   To design and develop a unidirectional Yagi-Uda antenna for 4G LTE coverage enhancement.

II.   To analyze the effect of the changes in width of the antenna elements towards the antenna.

III.   To evaluate the performance of the antenna in transceiver system.

1.4   Work Scope

The work scope of the project is to understand, design, analyze, and develop the implementation of a unidirectional Yagi-Uda antenna for enhancing 4G LTE coverage in areas with a weak internet signal. In this endeavor, the 4G antenna is made up using a Yagi-Uda antenna with rectangular elements made from recycled biscuit cans. The Yagi-Uda antenna is known for its directivity, high gain, and ample bandwidth, is well-suited for 4G LTE enhancement applications.

To serve as the internet source, a built-in SIM card router is utilized, offering a more cost-effective option compared to DSL modem routers. In this setup, the Yagi-Uda antenna directly captures signals from the cell tower, establishing communication with the 4G LTE Router via coaxial cable based on the tower's frequency band. This process ensures the generation of a reliable 4G LTE signal, allowing users to connect to the internet upon inserting a SIM card into the 4G LTE Router.

Accurate disk sizing, aligned with calculated dimensions, proper element spacing, and careful coaxial cable selection contribute to achieving the desired frequency, covering Band 7 at 2.6GHz. This optimized antenna design is scrutinized using CST software, where adjustments to element width are made to obtain the best simulation results. The chosen antenna, exhibiting optimal simulation outcomes, is then fabricated.

To enhance signal performance, the antenna is strategically positioned outdoors to increase directivity and gain. As a result, the implemented system provides a dependable, cost-effective, and efficient 4G LTE enhancement solution, improving the existing 4G LTE signal in areas with weak internet connections to a robust 4G LTE connection.

1.5   Thesis Organization

The thesis consists of five chapters, with each chapter presenting comprehensive details related to the project. The information pertaining to this project has been delineated in each chapter of the report, as outlined below:

Chapter 1: This chapter provides a concise project introduction. It includes discussions on the evolution of existing methods to recognize the system's

development. The chapter elaborates on the problem statement, objectives, scope, and overall project outline, offering a clear and thorough explanation.

Chapter 2: This chapter explores literature sources and journal articles relevant to the Unidirectional Yagi-Uda Antenna for 4G LTE coverage. It encompasses a review of the current scenario, theoretical foundations, and an overview of the system. The primary emphasis of this chapter is on the Yagi antenna as a unidirectional antenna and its underlying theory. Additionally, it underscores the problems and obstacles associated with 4G LTE mobile applications in specific geographical areas.

Chapter 3: This chapter highlights the sequential steps involved in the development of the 4G LTE Yagi-Uda Antenna functioning at 2.6GHz. It encompasses the utilization of pertinent formulas, software tools, and equipment for the antenna's design, development, and testing, aiming to fulfill the project objectives. Furthermore, it presents a project flowchart illustrating the applied methodology in the undertaking.

Chapter 4: This chapter presents the outcomes achieved during the project's completion within the semester. It encompasses the antenna design and simulation using CST Studio Suite, the analysis of coaxial elements width through parameter sweep on CST Studio Suite, and the optimization of the design for optimal performance. Additionally, it covers the overall performance assessment of the experimental setup for the Unidirectional Yagi-Uda Antenna, considering factors such as signal strength and speed in the transceiver system. This section will delve into the discussion of project results, considering simulations, laboratory testing, and field testing.

Chapter 5: This section will detail the conclusion and recommendations for the system. It encompasses a summary of the project, findings, and additional recommendations for enhancing the project.

CHAPTER 2

BACKGROUND STUDY

2.1   Introduction

The overall ideas and theories behind the Unidirectional Yagi-Uda Antenna for 4G
LTE Coverage Enhancement system are the main emphasis of this chapter. This
chapter's main objective is to make recent related studies more understandable. This
chapter covered the ideas and theories applied to the project's issues. Case studies,
articles, and journals are the primary sources of knowledge. They were picked based
on how well these resources' project scopes matched.

2.2   Review of Current Situation

Along with the anticipated nationwide rollout of 5G at an estimated 80% by year's
end, Communications and Digital Minister Fahmi Fadzil stated that the ministry would

continue to solve concerns relating to the current 4G network coverage. According to him, many communities continued to rely on the 4G network despite the nationwide launch of 5G. This is due to the ministry's ideals where there is no one left behind in the network development. Despite the launch of 5G, there are numerous villages out there considers that 4G network is crucial. So, in addition to the estimated 80% 5G network coverage by the end of the year, the government is dedicated to addressing the concerns with the 4G network coverage [2].

He claimed that as of May 2023, 96.92% of the nation was covered by the 4G network, although that percentage reflected coverage from all network providers taken as a whole. The minister have instructed the Malaysian Communications and Multimedia Commission to look into resolving the issue (on the 4G network coverage) and also on the 5G rollout. The current 4G network coverage in Malaysia is 96.92%, that is almost 100%, but the reality is that there is no single network provider that has that amount of network coverage [2].

Although people expect to have coverage everywhere when they pay their telecoms provider for network service, this is not the case. Consumers expect to have connections everywhere when they pay RM50 or RM100 for their network services. The government aims to put a stop to network coverage concerns if the prime minister is serious about ending extreme poverty for everyone [2].

It can be concluded that despite the wide 4G coverage nationwide, the telecom provider coverage are limited by areas due to limited infrastructure. Therefore, there is a need for an antenna that can enhance the 4G signal coverage at anytime and anywhere.

2.3   Theory

2.3.1   Mobile Wi-Fi in rural areas

The characteristics of Internet access in populated areas outside of towns and cities are referred to as rural Internet in Figure 2.1. Villages, hamlets, farms, and other remote residences are home to people. Rural Internet access may be challenging due to hills and other terrain features. Since most of these lines only serve a few customers, telecommunications firm maintenance and repair periods have slowed, and it is unlikely that they would upgrade to create advanced quality standards. Due to the lack of infrastructure for fiber optic internet connections in rural areas, accessing dependable high-speed internet there often involves more work than in major cities. Developing an ISL was exceptional since it requires subsidies to ensure the fiber is cost-effective. Therefore, high-speed internet expansion was restricted even though rural communities already possess cable, DSL, satellite, hotspot, hybrid fiber-coaxial, or fiber connection choices, despite increased funding for rural broadband [1].
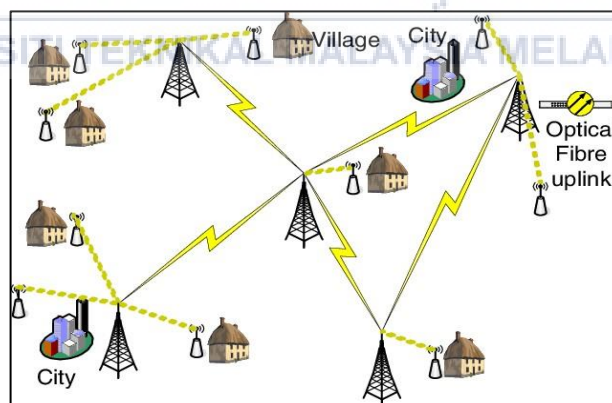
Figure 2.1: Example of Wi-Fi rural network.

2.3.2 Antenna in electromagnetic concept and principle

A significant component of a wireless LAN system is the Antenna. Antennas are devices that transmit or receive electromagnetic waves. If an antenna receives a signal, it converts the incident electromagnetic waves into electrical currents; if it is transmitting, it does the opposite. Antennas are designed to radiate or receive electromagnetic energy with radiation and polarization properties suited for their specific applications. Wireless data transfer modifications enabled an improvement in the data transmission rate of up to 100 Mbps for highly mobile users, for instance, those taking a train or driving, and up to 1000 Mbps for moderately mobile users under the LTE-Advanced and Wireless MAN-Advanced standards (WiMAX) [3].

Generally, the Yagi antenna, also known as a Yagi-Uda Antenna, is a form of an antenna array that radio communication operators commonly employ. It could be used as a television antenna, to receive radio signals emanating from space, and as a cellular antenna. It may be used for communications on frequencies ranging from short waves to microwaves, embracing the spectrum from very high frequency (VHF) to ultra-high frequency (UHF) [4]. The First equation defined wavelength in Equation (2.1) below, where the speed of light, c, is 3×108 m/s and frequency, f, represents the chosen operating frequency band of the Antenna. This parameter is vital in determining the length of elements in the Antenna.

$$\lambda_0 = cf \qquad\qquad\qquad (2.1)$$

2.3.3   Radiation pattern of Yagi antenna

Yagi antenna is created by driving a basic antenna, often a dipole or dipole-like antenna, and shaping the beam with a carefully selected sequence of non-driven components with tightly regulated length and spacing. Yagi antenna is made up of three fundamental components, which are the driven element, reflector and director. The driver is the only active element activated by a signal, while the reflector(s) and director(s) re-radiate by reflecting and directing the signal, respectively. As a result, both the reflector(s) and the directors are considered parasitic elements [5] [6].

Every parasitic element's length, which is the reflector and number of directors, varied from the resonant value of the half wavelength. If the length is more than 15%, the element exhibits inductive properties and acts as a reflector. Suppose the length is shortened by 5%. In that case, the elements develop capacitive properties and are referred to as directors because they appear to steer radiation in the direction of the driven polarity toward the director [7] [8]. A driven dipole alone with a director can be improved by changing to the reflector and a director on opposing sides of the driven dipole, which increases the gain up to 6dB [9]. By comparing the backward wave in Figure 2.2 and Figure 2.3, the longer reflector produces a backward wave which essentially cancels the wave from the driven element. Hence, the gain can be enhanced by adding more elements which also increases the gain, directivity, and efficiency [10].
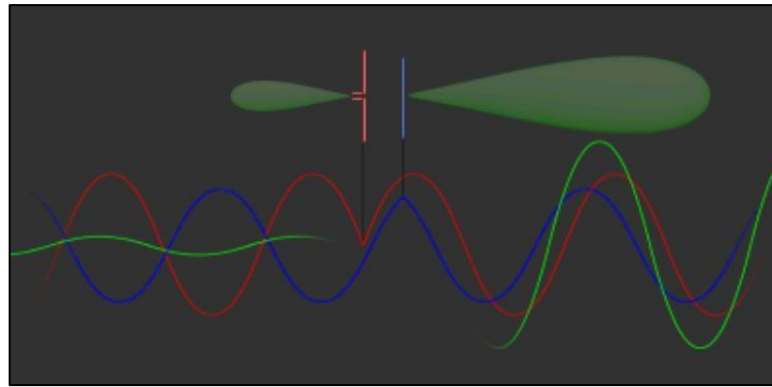
Figure 2.2: Two-element array of a half-wave resonant dipole as a parasite.
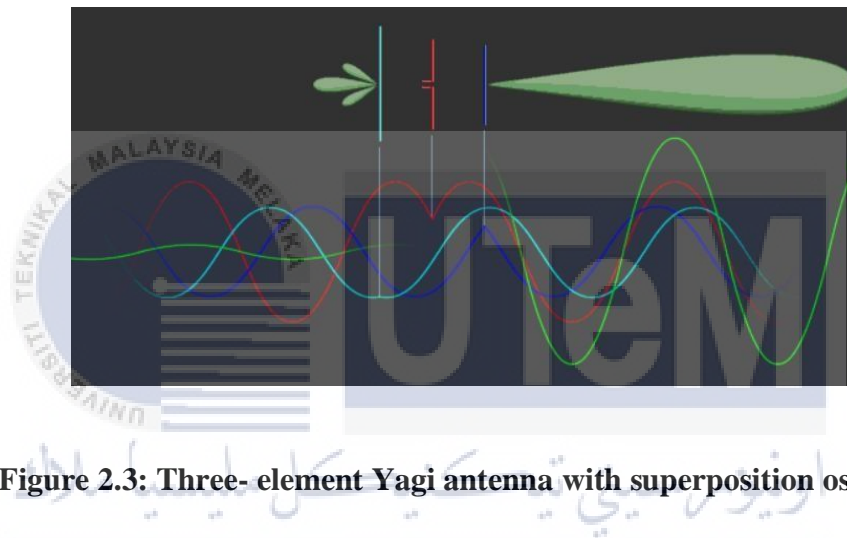
Figure 2.3: Three- element Yagi antenna with superposition oscillation.

Figure 2.4 shows a Yagi with one reflector (the bar behind the driving antenna) and 14 directors (the bars in front of the driven Antenna). Figure 2.5 shows this setup Yagi antenna produces a gain of roughly 15dBi with an azimuth and elevation plane beamwidth of about 36 degrees. This is a frequent characteristic of Yagi antennas. Because these antennas are frequently constructed to be rotated for either horizontal or vertical polarization, having the same 3dB beamwidth in either plane is a useful characteristic.
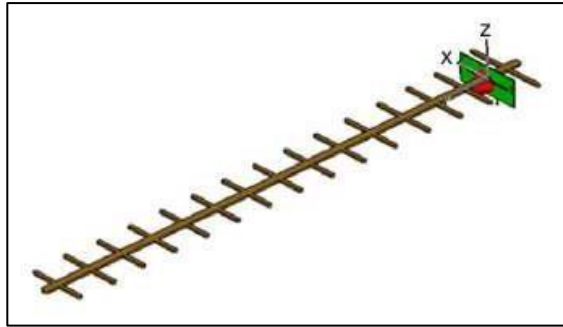
Figure 2.4: Yagi antenna model
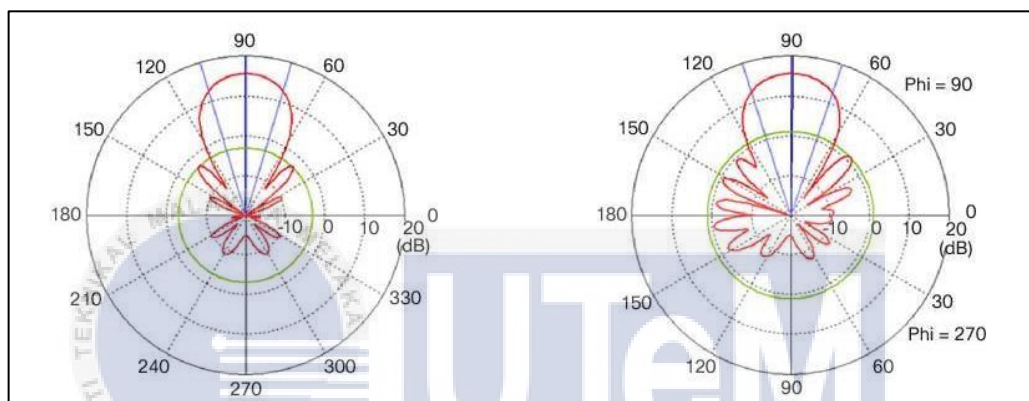
Figure 2.5: Yagi antenna azimuth and elevation plane pattern

The gain and radiation pattern with different spacing variations between elements, number of directors, folded active element feature and radius of the reflector. In the case of operating frequency at 300MHz [7], the simulation showed that by decreasing the space between elements from 0.4λ to 0.1λ, the gain value of the Yagi-Uda antenna increases from 8.66dB to 12.32dB. Meanwhile, the radiation pattern becomes narrower, which proves that the Antenna with less spacing between elements has higher directivity and gain. Additionally, when the number of directors was increased from 1 to 5 with the same length and spacing between elements, the antenna gains and directivity increased, yielding 16.03dB of maximum gain and a narrower radiation pattern. The gain for operating frequency at 2.4GHz increases when the spacing

between elements increases. However, when the spacing of elements decreased between 0.025m to 0.0125m, the gain decreased as the minimum space of 2.4GHz was at 0.2m. The gain and directivity also increased when the number of directors increased from 4 to 6.

2.4   Dimension Changing Effect on Antenna.

In a conventional design dedicated for Wi-Fi application, observing that the antenna size decreases with increased operational frequency, the design for a 2.4GHz Yagi-Uda antenna is limited to three elements. This limitation stems from the requirement that each element's length should decrease by 5%. Consequently, adding more directors to enhance gain is not feasible. Instead, consideration was given to closely spacing the elements at 0.2λ intervals. In an attempt to modify the 2.4GHz Yagi-Uda antenna, experimentation involved increasing the radius of reflectors. The graph illustrates an initial increase in gain, peaking beyond a 6mm radius, after which a decline is observed. Subsequently, adjustments were made to the design by increasing the reflector radius while maintaining close spacing and a compact size. The resulting radiation pattern at 2.4GHzindicates a gain of 12.54dB [7].

Following the adjustment, the ground plane length increases incrementally from 48.9 to 56.9 mm, with a 2mm increment in each step. In Figure 9, the return loss (S11) is illustrated, indicating a reduction in magnitude and a leftward shift for the first resonant frequency as the ground plane length (Lg) increases. The return loss also exhibits slight variations for the higher resonant frequency, with a significant leftward shift from 2.6 GHz. Front-to-back (F/B) ratio and directivity were investigated for both frequencies, and Table 2 summarizes the study's results.

In the Quasi Yagi 4G LTE antenna application at 1.80 GHz, the F/B ratio initially increases from 13.47 to 13.61 dB, then decreases to 12.76 dB with the increase in Lg from 48.90 mm to 56.90 mm. Similarly, the directivity at 1.80 GHz increases from 6.63dBi to 6.74dBi and then decreases to 6.5dBi. For the resonant frequency of 2.60GHz, the F/B initially increases and later decreases, while directivity decreases with an increase in the length of L_g. The decrease in F/B is attributed to the growing back lobe of the radiation, as the partial ground plane acts as the reflector element.

In this study, the length of the driving element is varied from 63.20 to 71.20 mm. Figure 10 illustrates that the first resonant frequency significantly changes with the variation in driven element length (L_{dr}), while the second resonant frequency remains almost fixed at 2.60 GHz. The quasi-Yagi antenna resonates at 1.80 GHz and 2.60GHz, providing suitable bandwidths and reflection coefficients for the desired LTE spectrum. The reflection coefficients are -67dB and -35 dB at 1.80GHz and 2.60GHz, respectively, for a driven element length of 71.20 mm [11].

2.5   Comparison of Previous Work on Antenna for Wireless Communication Application

Table 2.1 compares the previous work and research done in the past 5 years regarding developed antenna for wireless communication applications.

Table 2.1: Comparison of previous work on Antenna for wireless communication application

Ref	Antenna Type	Application	Resonance Frequency	S_{11} (dB)	Gain (dB)	Directivity (dBi)	Efficiency (%)

[5]	Quasi-Yagi	4G LTE	1.85GHz, 2.64GHz	-50.44, -35.67	6.76	6.79	83.05
[6]	Planar Yagi	4G LTE	2.6GHz – 4.3GHz	-25	8.31	9.93	83.69
[7]	Conventional Yagi	Wi – Fi	300MHz, 2.4GHz	-	15.32, 12.54	-	-
[10]	Rectangular Microstrip Patch Yagi	5G	28GHz	-41.32	8.931	9.773	82.37
[12]	Yagi Biquad	4G LTE	2.1GHz – 2.4GHz	-26.44	9.23	-	-
[13]	Two Dipole Array	4G LTE	1.7GHz – 2.8GHz	-32.5	8.1	-	-
[14]	Eight-Element Array	5G	21GHz – 23.5GHz	-30	12.5	13.1	90
[11]	Dual-band Quasi Yagi	4G LTE	1.8GHz, 2.6GHz	-65.23, -31.55	6	8.3	73
[15]	Quasi-Yagi Slotted Array	5G	28GHz	-32	11.09	-	-
[16]	Dual-band Planar	4G LTE	Mid: (1.427GHz – 2.69GHz) High: (3.4GHz – 3.8GHz)	-32	Mid: 3.4 High: 6.1	-	Mid: 90 High: 88
[17]	Circular-disk Yagi	4G LTE	1.8GHz	-48.82	11.15	-	-

[18]	Circular-disk Yagi	4G LTE	1.8GHz	-42.68	11.17	-	-
[19]	Wideband Microstrip Patch Antenna	5G	3.5GHz – 5GHz	-14.287	-0.9762	2.07	-
[20]	Minkowski Fractal Yagi	4G LTE	1.8GHz	-28	6.48	-	-
[21]	A 2×2 Inset Feed Circular Patch Antenna Array	4G LTE	1.8GHz	-24.78	6.55	-	-
[22]	Microstrip Patch	4G LTE	1.8GHz, 2.1GHz, 2.6GHz	-14, -23, -18	-	-	-
[23]	Eight-Port MIMO Antenna	4G LTE	2.6GHz	-23	-	4	-
[24]	Triple band MIMO dielectric resonator	4G LTE, 5G	1.8GHz, 2.6GHz, 3.6GHz	-17, -19, -21	5.5, 5.9, 6.9	-	-
[25]	MIMO Amer Fractal Slot Antenna	3G, 4G LTE, WLAN, WiMAX	P1(1.5-19.2, 25-37.2) GHz P2(1.4-19, 20-35.5) GHz	≤ -30	1.3 – 6.3, 1.2 – 6.3, 1 – 6.2, 1 – 6.3	-	50 – 85, 53 – 85, 54 – 80, 56 – 82

			P3(1.4-29) GHz P4(1.6-21, 22-37)GHz			
[26]	Dual-band Microstrip Patch Antenna	4G LTE	1.8GHz, 2.6GHz	P1 (-13.5, -13.323) P2 (-14.806, -13.462) P3 (-13.902, -13.281) P4 (-14.806, -13.461)	3.969, 3.22	-	-
[27]	2x1 Truncated Corner Microstrip Array Antenna	4G LTE	2.3GHz	-18.171	3.963	-	-
[28]	Microstrip Patch Antenna Array	WLAN, 4G LTE	2.5GHz	-27	4.84	4.97	80

CHAPTER 3

METHODOLOGY

3.1   Introduction

The overall ideas and theories behind the unidirectional Yagi-Uda Antenna for 4G

LTE coverage enhancement application are the main emphasis of this chapter. This

chapter's main objective is to make recent related studies more understandable. This

chapter covered the ideas and theories applied to the project's issues. Case studies,

articles, and journals are the primary sources of knowledge. They were picked based

on how well these resources' project scopes matched.

3.2   Flowchart
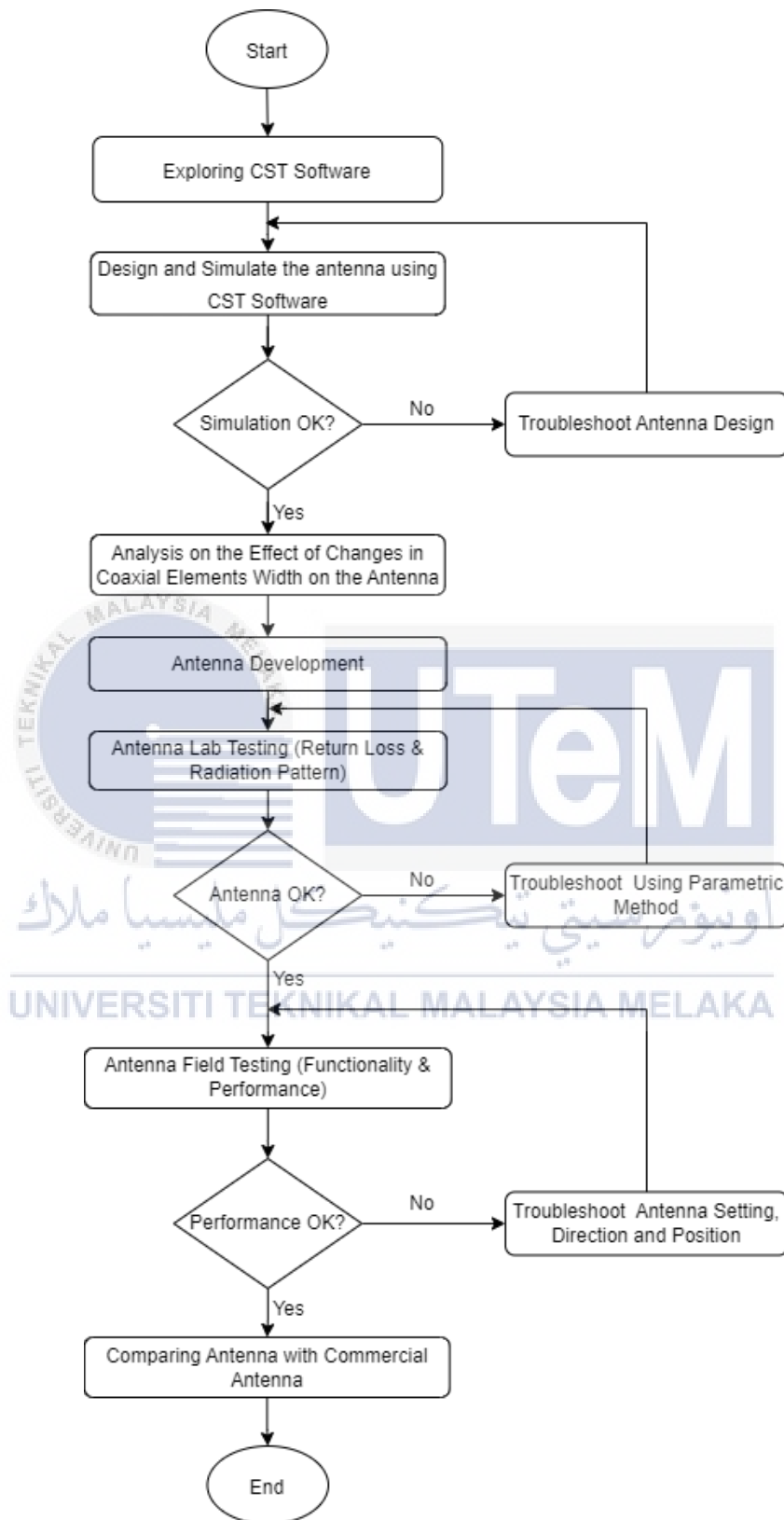
Figure 3.1: Flowchart of the project.

3.3   Process Explanation

The explanation of the flowchart, as shown in Figure 3.1, is as explained below. It displays the project's flowchart and the methods used to complete the project. It gave a thorough step-by-step explanation and illustrated each step's subtopic.

3.3.1   CST Software Exploration

Designing, analyzing, and optimizing electromagnetic (EM) components and systems can be done with the help of the high-performance 3D EM analysis software suite known as CST Studio Suite® [29]. It is a software used specifically to design, simulate and optimize the antenna in this project. As a first time user of the software, there is a lot to learn on how to use the designing tools, the simulator, the optimizer and other features of the software to ensure the desired outcome is obtained.

3.3.2   Design and Simulate Antenna Using CST Software

The three main elements of developing the 4G disc-Yagi antenna are the reflector, driven element, and directors, as shown in Figure 2.7. This project used elements made of steel from biscuit tin to develop a low-cost metallic disc as the elements. The number of directors used was six, as the greater the number of directors used for the Antenna, the greater increase in gain as well as decreasing the bandwidth [12]. To operate efficiently, the Antenna should be within 10% bandwidth or ±5% of the operating frequency [30]. In this case, the operating frequency ranges between 2.47 GHz to 2.73 GHz for the 4G antenna designed for 2.6 GHz.

The size of the disc and the spacing between elements can be seen in Figure 2.8. The spacing between elements will manipulate the gain for the 4G disc-Yagi antenna in which the spacing between directors is maintained between 2.2cm to 2.6cm.

Meanwhile, the spacing between the reflector to driven element' and driven element to the first director is 0.5cm and 0.2cm, respectively.
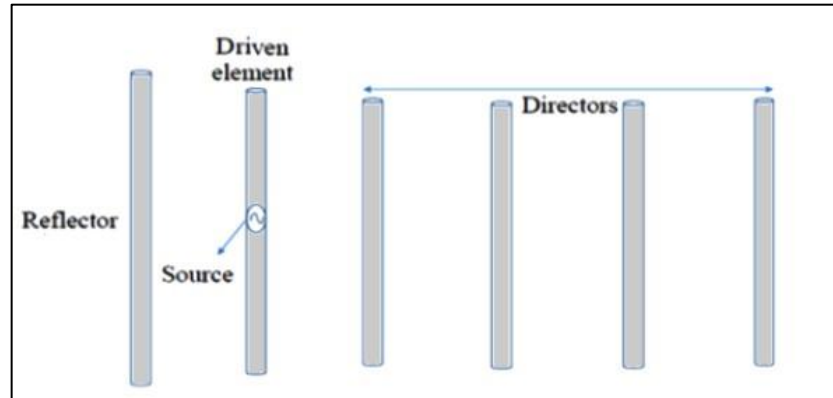
Figure 3.2: Elements in the LTE Yagi antenna

The final design of the disc-Yagi Antenna is obtained after using the parametric method. The parameter in the initial design from the theoretical design formulation was manipulated until the desired output could be obtained. Below is the calculation for theoretical design formulation.

$$f = 2.6\ GHz \tag{3.1}$$

$$\lambda = \frac{c}{f} = \frac{3 \times 108}{2.6\ GHz} = 0.1154\ m \approx 115.4\ mm \tag{3.2}$$

Diameter, L calculation:

$$L_{dipole} \leq \frac{\lambda}{2} \tag{3.3}$$

$$L_{reflector} = 5\% > L_{dipole} \tag{3.4}$$

$$0.4\ \lambda < L_{director} < 0.45\ \lambda \tag{3.5}$$

Distance between reflector to dipole,

$$0.1\,\lambda < S_{rd} < 0.25\,\lambda \tag{3.6}$$

Distance between director to director,

$$0.1\,\lambda < S_{dd} < 0.3\,\lambda \tag{3.7}$$

3.3.3 Analysis on the Effect of Changes in Coaxial Elements Width of the Antenna

During the designing process of the antenna in CST Suite Software, the width of the coaxial elements of the antenna for theoretical and calculations designs are varies within its range as in (3.3), (3.4) and (3.5). Simulation for all variations are run in order to plot the s-parameter and radiation pattern to find the return loss and the gain of the antenna consecutively. The results are then compared by evaluating the best return loss and the highest gain to find the best parameter for fabrication. The design with the best result is then proceed with the development process.

3.3.4 Antenna Development

The antenna development began with researching the features suitable for the chosen frequency band of 2.6GHz. Paper disks were then drawn using a protector and ruler, and their outlines were traced onto a biscuit can. Cutting the can was done with a metal cutter due to its hardness. Safety precautions were taken to prevent injuries during this process.

To ensure precise measurements, the dimensions of the metal discs were rechecked with a regular ruler. Holes were drilled in the middle of each disc using an electric driller with a 6.5 mm bit, which was slightly larger for easy installation on the metal rod. For the reflector, two additional holes were drilled 2 mm away from the center to accommodate the SMA cable. Prior to using the 6.5 mm bit, smaller holes were drilled for precision using a 3.0 mm bit.

Safety was a priority during drilling, considering the potential electrical hazards. The drill plug was turned off when changing the bit to avoid current flow. Precautions were also taken to ensure the bit was tightly attached to the chuck. Drilling was carried out on a wooden block for safety.

After drilling, a small hole was made in the active element disc to allow the SMA cable to pass through. Soldering work was done carefully, with the pin soldered on the active element and the braided shield soldered on the reflector for grounding. Safety measures were observed to avoid inhaling fumes and prevent burns.

The discs were finally installed on the metal rod with specified distances as per the design. Careful installation was crucial to prevent damage to the discs and avoid injuries from their sharp edges. Distances between elements were confirmed with a regular ruler before proceeding with testing.

3.3.5   Antenna Lab Testing

The purpose of this lab test is to identify the return-loss, 2D radiation pattern, 3D radiation pattern, efficiency and gain of the antenna developed. Return-loss testing was carried out using PNA-X Network Analyzer by Agilent Technology as in

Figure 3.3. Before testing, the equipment need to be calibrated with N4433A Electronic Calibration Module as shown in Figure 3.4 to ensure the accuracy of the result. Then, the range frequency is placed at the range of 2GHz to 3GHz where it is easier to monitor the return loss at desired frequency which is 2.6GHz.
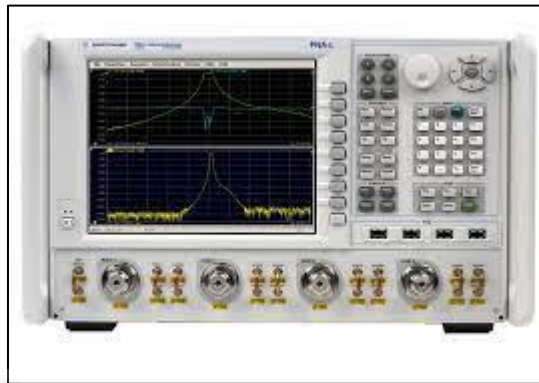
Figure 3.3: PNA-X Network Analyzer
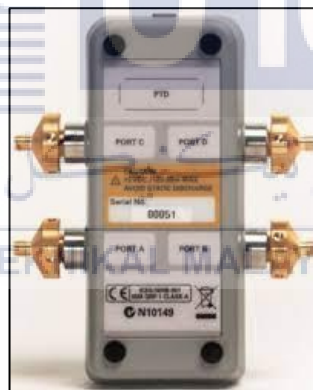
Figure 3.4: N4433A Calibrator

When the return-loss test meets the specification needed, the lab test is taken to the next step which is in the anechoic chamber. The antenna setup in this chamber can be seen in Figure 3.5 where it includes RF transmitter system, receiver antenna, positioning system and reference antenna. This test is important as the condition are more controlled than outdoor testing. The test taken place in this chamber involve radiation pattern in 2D and 3D, efficiency and gain which take several hours to

complete. The most needed result is the 2D, gain and efficiency as the 3D result is a bit different from the theory. Therefore, it requires higher skill in understanding positioning system of the testing done. However, it is essential to execute the 3D radiation test in order to obtain the antenna gain and efficiency.
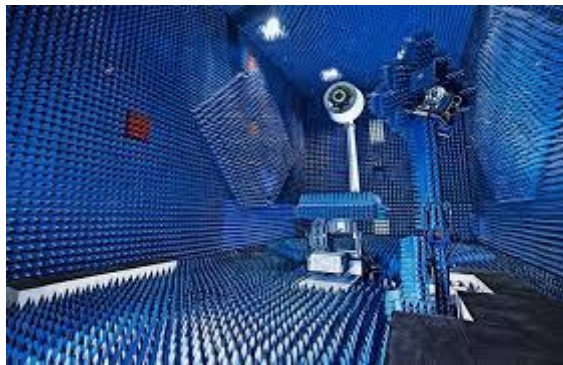
Figure 3.5: Anechoic Chamber.

Based on Figure 3.6, the antenna testing was performed using reference antenna, a dual-polarized horn antenna for measuring horizontal and vertical polarization simultaneously and antenna under test which is the designed 4G antenna. As shown in Figure 3.7, the testing was conducted by attaching the antenna to the positioner in which will control the rotating of the antenna under test to measure the radiation pattern. The radiation pattern presents directivity, gain, electric field, or radiation vector.
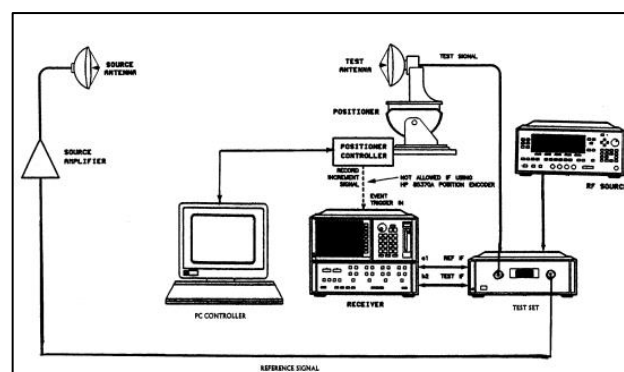
Figure 3.6: Illustration of antenna testing in anechoic chamber.
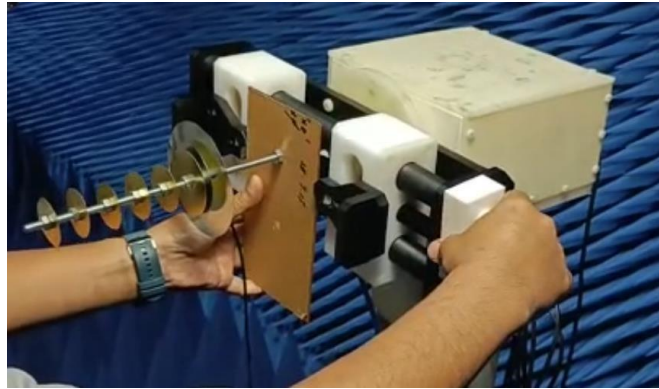
Figure 3.7: 4G LTE antenna is clipped to the positioner

3.3.6   Antenna Field Testing

Field test was carried out after accomplished the aim of lab test. For field testing, the interconnection of the Disk-Yagi antenna in installation process is shown in Figure 3.8. The router containing prepaid sim card with data plan is connected to disc-Yagi antenna using the coaxial cable, LMR240 with approximately 15 m long. This is to ensure the antenna can be positioned at the best possible location with less interference. Therefore, the length of coaxial cable is depending on the suitable distance for its application. Additionally, to get the best output from this testing, the type of coaxial cable was considered to avoid signal loss during signal transmission. LMR240 was chosen because it had the least attenuation if compared to RG58.

Furthermore, any local service provider is chosen as it offers the most affordable monthly data plan. Then, the antenna should be adjusted toward the nearest base station transmission, BTS that serve band 7 to improve the internet connection.

Figure 3.8: Block diagram for project

In performing the field test, there were two settings should be done before installing the antenna. Firstly, the antenna setting of the modem was configured to two port external antenna. This configuration can be accessed by browsing the modem's default IP address which is http://192.168.8.1/. Logging into this modem will allow the user to do any changes especially on antenna setting and the network preferred mode setting in Figure 3.9 and Figure 3.10 respectively.
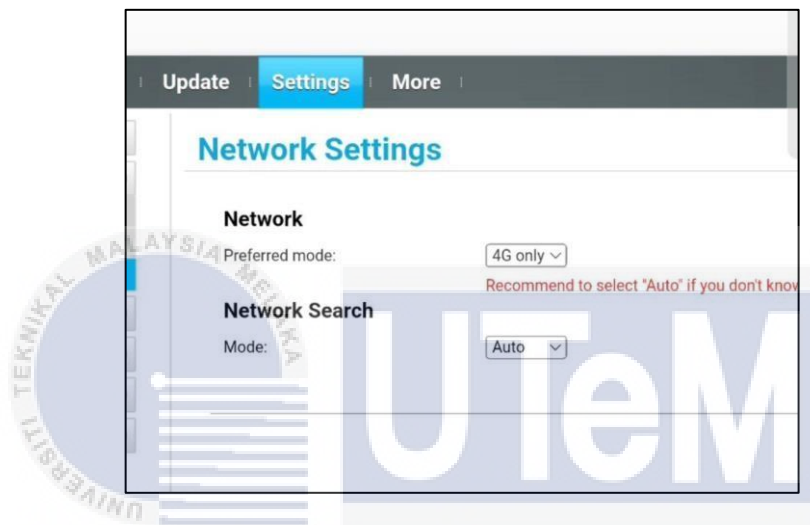
Figure 3.9: Network setting in modem configuration setting.
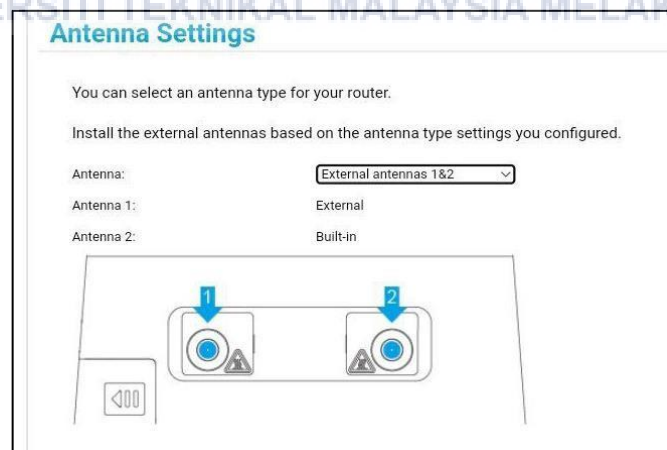
Figure 3.10: Antenna setting in modem configuration setting.

Then, the base tower is located using CellMapper.net from Figure 3.11, green network logo indicates the available base tower while the red is the non-functional base. From the logo itself will show the band service of the base tower. Therefore, the nearest base tower that cover the testing location with band 7 was chosen. The tower information is displayed when double clicking on the tower. From this information, approximate location of the tower was discovered using Google Maps by comparing the testing location terrain. It is also useful as the device with built in GPS such as mobile phone shows the current position direction in the Google Maps.

Thus, the direction toward base tower can be more accurate.
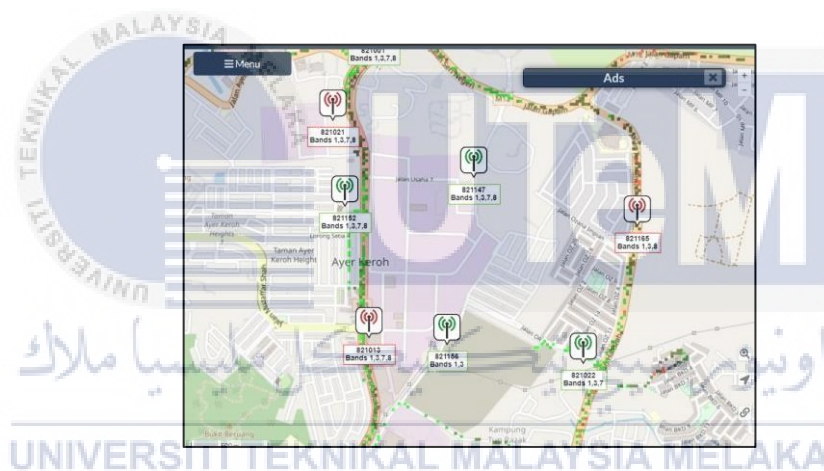
Figure 3.11: Base station in CellMapper.

Knowing the base tower location, the antenna was adjusted according to the finding and the field test parameters were tested. There are two applications used for field testing which are the Speed Test and Huawei Manager app as in Figure 3.12. In Speed Test, the parameter tested were the speed download and upload. Next, the parameter tested in the Huawei Manager app are RSSI, RF-MARGIN, 4G-RSRP, 4G-RSRQ and 4G-SINR.
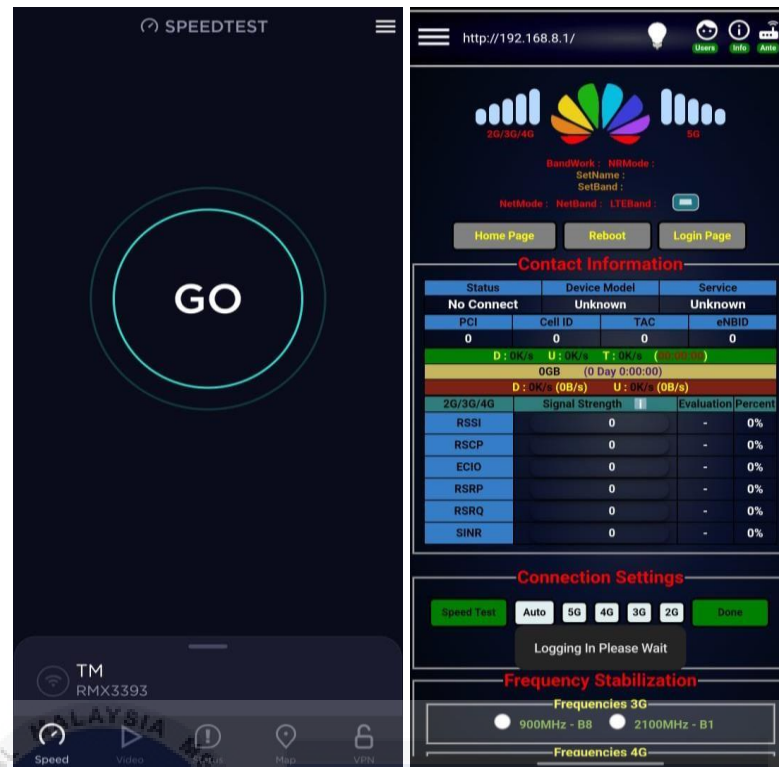
Figure 3.12: Speed Test by Ookla and Huawei Manager application (from left).

3.3.6.1 Hardware used for Field Testing

In this part, the most crucial consideration of the hardware used are the router and coaxial cable. These components are the major part in field testing to get desirable outcome.

3.3.6.1.1 Huawei Router B310As-852

Huawei B310As-852 router allows the user to use their data plan as a Wi-Fi or Ethernet. With the dimensions of 181mm (H) x 126mm (W) x 70mm (D), it only takes a little space. Referring to Figure 3.13, it has four icons that lit to indicate the status of the router. Starting from left, the first icon shows power on. The following icon indicates the status of the connected network, the status of Wi-Fi network, status of

Ethernet connecter and operator's signal bars. Moreover, it also comes with two external antenna that uses SMA female jack [31].
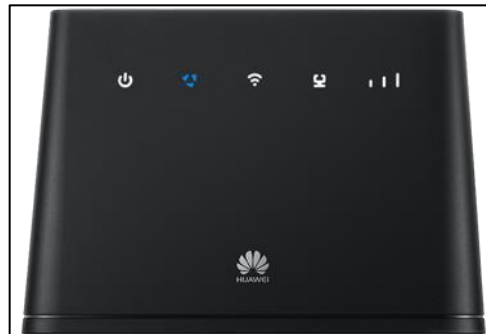
Figure 3.13: Huawei router B310

The best quality and affordable router that can be chosen from was Huawei B315 LTE CPE and Huawei B310 LTE CPE. The B315 and B310 routers are both wireless gateway that combines LTE and high-speed Ethernet uplink connectivity, allowing users to access data and voice services in a flexible and diverse manner [32]. From the comparison in the table in Appendix B, there were no prominent differences between both routers. Although B315 was an upgraded version of B310, the features offered in model B310 is sufficient. Thus, B310 was chosen for this project.

Apart from that, each model has a variation to accommodate multiple LTE frequency bands from various network operators. B310 and B315, both have four variant models where B310 variants are, B310s-927, B310As-852, B310s-22, and B310s-518 while B315's variants are B315s-22, B315s-607, B315s-608, and B315s-936. By referring to Table 5 in supported 4G LTE frequency bands, the selected variant is B310As-852. It supports Malaysian ISPs with the required frequency band which is band 7 (2600MHz). Hence, the B310As852 was used for this project.

3.3.6.1.2 Coaxial Cable
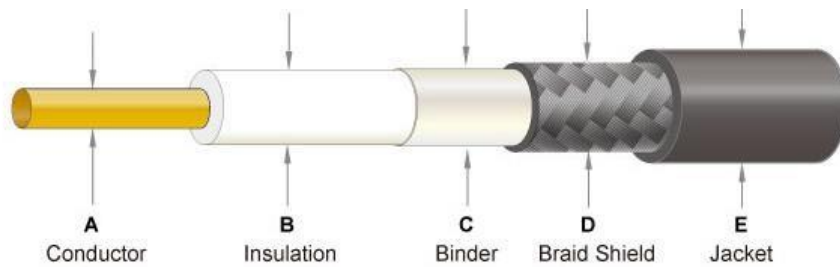
Figure 3.14: Structure of LMR240

LMR-240 coaxial cable is a product in demand that is widely recognized as the industry standard with extremely low loss, flexible, low cost and lightweight coaxial cable. Referring to Figure 3.14, it consists of four layers of materials which made up of a core conductor, an insulating material layer, a mesh fabric shielding layer, and an outside isolation material layer [33]. It is used for a wide range of RF applications. Generally, all LMR standard coaxial cable jackets were made of PE jacket with UV resistance. This specification was the reason the coaxial cable suitable for outdoor use since it has high resistance towards harsh environment [34]. It is mainly use for radio frequency transmission line compared to transmission of electrical power. Moreover, LMR240 can carry higher frequencies than conventional cable.

Following, the term "RG" stands for "Radio Guide," and originates from World War II. The RG Cable was used for US military standards since it was formerly a unit indication for bulk radio frequency. The RG-6 cable is generally used for transmitting cable and satellite signals for home and business installations. This coax cable is thin and flexible, making it ideal for wall or ceiling installations, and it is still the favored choice for relaying cable television signals. The cable contains a larger conductor,

which improves signal quality, as well as thicker dielectric insulation, which makes it less prone to transmit harmful electric currents [35].

Comparing LMR240 with RG6 based on the table in Appendix C, it is important to use coaxial cable with an impedance of 50Ω instead of 75Ω. This is because 50Ω line is utilized for high frequency range while 75Ω frequency range is more suitable for audio or video signal in TV applications. Considering the core thickness, it is better to have a thicker core as it will offer lower loss. The low loss is a desirable characteristic in a coaxial cable to minimize the signal loss. Therefore, LMR240 was chosen for this field testing [35].

CHAPTER 4

RESULTS AND DISCUSSION

4.1   Introduction

The overall results of the simulation, lab test, field test and antenna performance comparison of the Unidirectional Yagi-Uda Antenna for 4G LTE Coverage Enhancement system are the main emphasis of this chapter. This chapter's main objective is to observe the functionality and the performance of the designed Unidirectional Yagi-Uda Antenna to serve its application in a transceiver system. This chapter covers the CST simulation of the most optimized design, lab testing and field testing result of the finished prototype. The outcome is discussed in this chapter.

4.2   CST Studio Suite Simulation Design and Analysis

The first major process of this project is the simulation process which is done using CST Studio Suite. The coaxial elements of both designs are varied and analyzed to obtain the best outcome.

4.2.1   Initial Design

This design is based on the optimal design parameters for a Yagi-Uda antenna operating at 2.6GHz. It is derived from the circular-disk Yagi-Uda antenna, where the dimensions of the elements are determined by the diameter. The performance metrics such as return loss, gain, directivity, efficiency, and half-power beamwidth (HPBW) were evaluated for this design.

4.2.1.1 Antenna Design

Figure 4.1 below shows the initial design overview of the rectangular-disk Yagi-Uda antenna using CST Studio Suite. The figures show the front-view, back-view and the perspective-view of the initial antenna design.

| **(a)** | **(b)** | **(c)** |
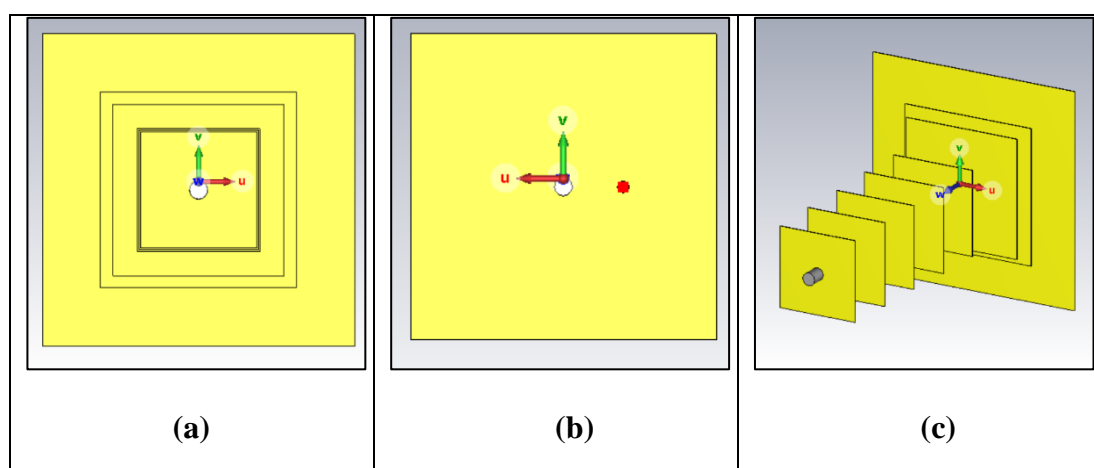
Figure 4.1: Initial design overview (a)front-view, (b)back-view and (c)perspective-view

The dimensions of the rectangular-disk Yagi antenna are presented in Table 4.1, where the width of each coaxial element matches its length, resulting in a square shape coaxial elements. The reflector disk has the largest dimension, followed by the driven element and directors. To enhance the antenna's gain and directivity, six directors were employed in this design. The rationale behind this choice is that an increase in the number of directors leads to higher gain and greater antenna directivity [18].

Table 4.1: Elements dimension of the initial antenna design

Components	Dimension (mm)			
	Width, W		Length, L	
Reflector	W_R	102	L_R	102
Driven Element	W_E	64	L_E	64
Director 1	W_{D1}	56	L_{D1}	56
Director 2	W_{D2}	40	L_{D2}	40
Director 3	W_{D3}	40	L_{D3}	40
Director 4	W_{D4}	39	L_{D4}	39
Director 5	W_{D5}	39	L_{D5}	39
Director 6	W_{D6}	38	L_{D6}	38

Figure 4.2 and Table 4.2 show the distance between the elements of the antenna. The distance between the coaxial elements were set uniformly to maintain the antenna stability. The spacing affects various parameters such as the impedance matching, radiation pattern, and overall efficiency of the antenna. A consistent and well-defined spacing helps in achieving a balanced distribution of electromagnetic fields between

the driven element, directors, and reflector, which contributes to the desired directional characteristics of the Yagi-Uda antenna. As shown in the table, the distance between the reflector and the driven element and the distance between the driven element and the director 1 were set at 5mm while the distance between the directors were set at 25mm. The distance was calculated by using (3.6) and (3.7).
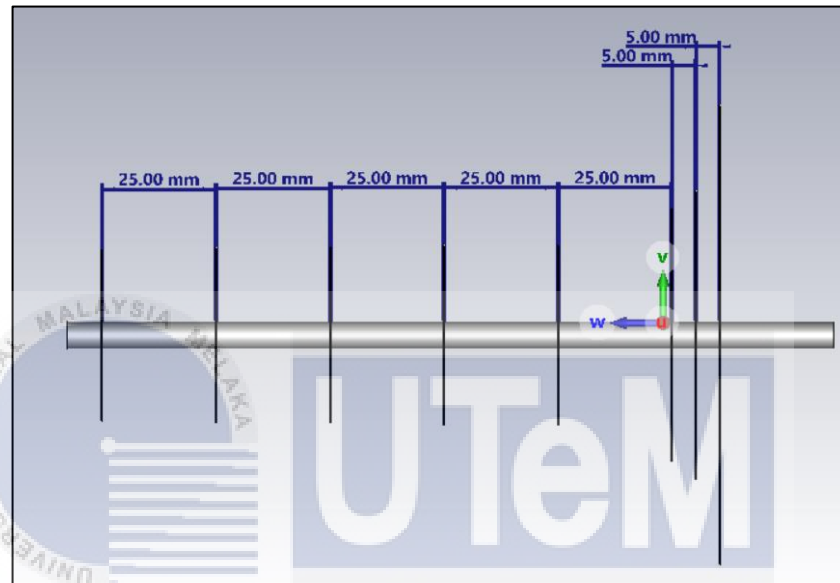
Figure 4.2: Distance between elements

Table 4.2: Distance between elements

Elements	Distance (mm)
Reflector to Driven Element, $S_{ref-dri}$	5
Driven Element to Director 1, $S_{dri-dir1}$	5
Director 1 to Director 2, $S_{dir1-dir2}$	25
Director 2 to Director 3, $S_{dir2-dir3}$	25
Director 3 to Director 4, $S_{dir3-dir4}$	25
Director 5 to Director 6, $S_{dir5-dir6}$	25

4.2.1.2 S-Parameter

Figure 4.3 and Table 4.3 below shows the return-loss obtained from the simulation run on the initial design. The initial return-loss obtained was at the frequency 2.1GHz (Band 1) and 2.3GHz (Band 40) which were not the desired frequency spectrum for this project. However, these two frequencies have good return-loss which were below -10dB as shown in the figure.
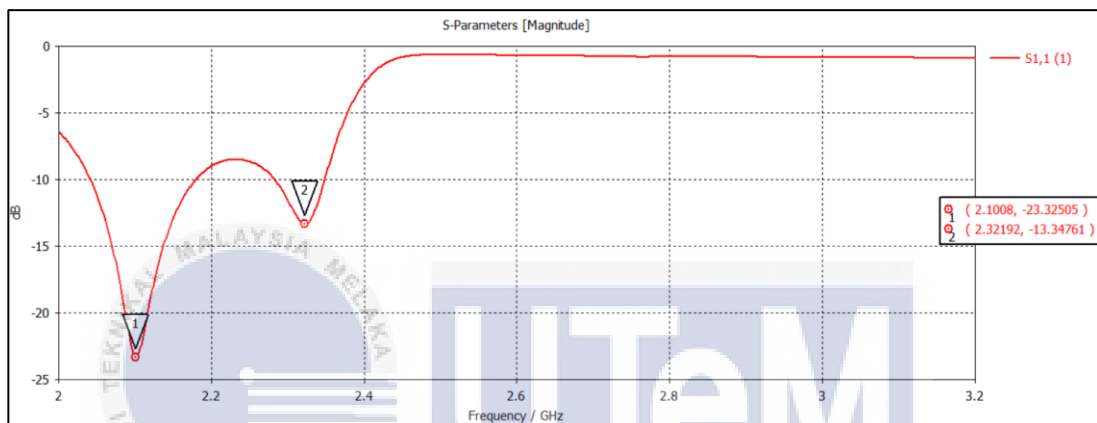
Figure 4.3: Simulated S11 for the initial design

Table 4.3: Return-loss measurement of the initial design

Frequency (GHz)	Return-Loss (dB)
2.1008	-23.32505
2.3212	-13.34761

4.2.1.3 Radiation Pattern of the Initial Design

The aim of this project is to develop a unidirectional antenna. Thus, the radiation pattern should be a unidirectional radiation pattern with one distinctive major main lobe and minor side lobes. Figure 4.4 below shows the radiation pattern of the antenna at 2.6GHz on the -plane (Phi=90). As shown in the figure, the radiation pattern

obtained was a bidirectional radiation pattern with two major main lobes and two side lobes. Therefore, the radiation pattern was not as desired for the project.
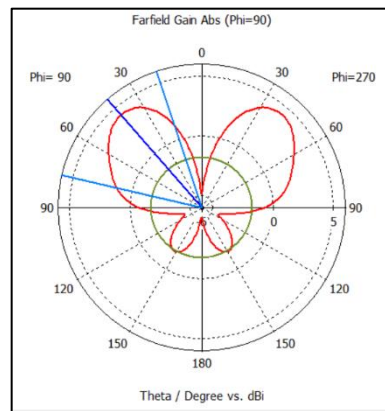
Figure 4.4: Radiation Pattern at 2.6GHz in Polar plot

Figure 4.5 below shows the 3D radiation pattern of the antenna at 2.6GHz. As depicted in figures (e) and (f), representing the right and left views of the radiation pattern, it is evident that the pattern exhibits the bidirectional radiation pattern. Consequently, the intended outcome was not successfully attained.
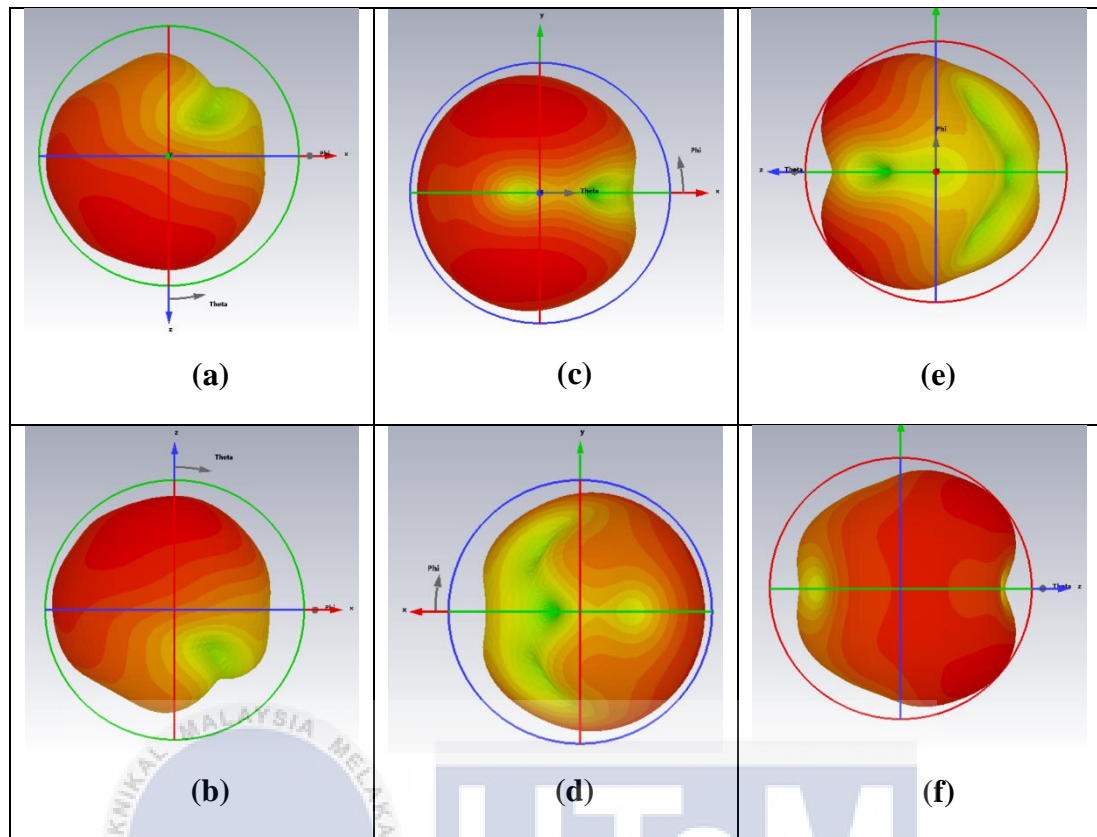
**Figure 4.5: 3D Radiation Pattern at 2.6GHz Overview (a)Top-view,
(b)Bottom-view, (c)Front-view, (d)Back-view, (e)Right-view, and (f)Left-view**

4.2.1.4 Gain, Directivity, Half Power Beamwidth, and Efficiency

Table 4.1 below shows the parameters measured at 2.6GHz throughout the
simulation in CST Studio Suite. The initial design exhibits relatively modest gain and
directivity, measuring at 4.278dBi and 4.392dBi, respectively. The target for this
project is a higher level of 10dBi, which is considered substantial, indicating a strong
emphasis on achieving elevated gain and directivity. The term "gain" refers to the
antenna's ability to focus or amplify signals in a specific direction, while "directivity"
pertains to its capacity to concentrate radiation in a targeted path. The intention is to
enhance these parameters significantly, aiming for a higher level of performance
characterized by a gain and directivity of 10dBi, which is regarded as high in the

context of antenna design. Moreover, the efficiency of this antenna design is notably limited, registering at a mere 14.74%.

Table 4.4: Antenna parameters measurement at 2.6GHz

Gain	Directivity	HPBW	Efficiency (Total)
4.278 dBi	4.392dBi	58.6°	14.74%

4.2.2 Antenna Design Analysis

In the antenna design analysis, variations were introduced by altering the width of the coaxial elements in the rectangular-disk configuration. This involved both increasing and decreasing the width of these elements. The purpose of these adjustments was to systematically assess the impact of changes in width on the antenna's performance metrics. Parameters such as gain, directivity, and efficiency were analyzed to understand how modifications to the coaxial elements influenced the overall behavior of the antenna. This approach allowed for a comprehensive examination of the antenna's sensitivity to width variations and provided insights into the optimal configuration for achieving desired performance characteristics.

4.2.2.1 Increasing the Elements Width

The width of the elements was gradually increased to reach 4mm. To understand how this change affected the antenna, a parameter sweep was conducted using CST Studio Suite. Sequences and parameters were defined in the Time Domain Solver, assigning each parameter to a different sequence. In this case, the parameters included the width of individual coaxial elements, such as the reflector, driven element, and six directors. This process resulted in eight sequences in total. The outcomes of the

parameter sweep were then compared to assess the impact of the width increment on the antenna design.

4.2.2.1.1 Increased Width Return Loss Analysis

Figure 4.6 below shows the comparison of the S11 plotted. In this analysis, a comparison was made among three designs that yielded the most significant outcomes, presented in a single graph. The S11 of the initial design was also incorporated into the plot to observe any potential improvements. In the graphical representation, the S11 of the initial design was represented by a red dash-dot line. The S11(10), depicted by a green solid line, was selected because the signal resonated at 2.3348GHz, exhibiting a favorable return loss of -17.1052dB, which is in close proximity to the desired frequency of 2.6GHz. The S11(22), shown as a blue solid line, was chosen due to its signal resonating at the least favorable frequency of 2.0036GHz, farthest from the desired frequency. Lastly, S11(199) was selected for its incremental behavior in each coaxial element, maintaining a good return loss despite not resonating at the desired frequency.
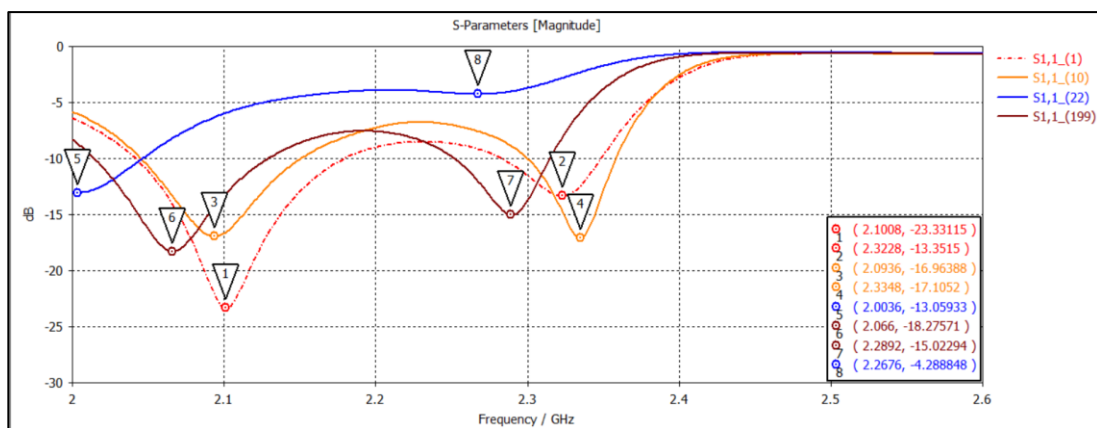
Figure 4.6: Increased width return-loss analysis

Table 4.5 below displays the chosen dimensions, selected based on the notable S11 results obtained during the parameter sweeping process. Specifically, the widths

corresponding to the three most significant S11 values were compared to the initial width.

From the figure and the table, S11(10) only increases the width of Director 3, W_{D3} with an increment of 4mm and manage to resonate at the frequency nearest to the desired. As for S11(22), the width increment only happened at the Driven Element, W_E with an increment of 4mm and it has the worst outcome compared to the rest of the S11 from the sweep. As for S11(199), each coaxial element has a width increment where the reflector's width increased 3mm, driven element's width increased 1mm, director 1 and 2 increased 1mm, director 3 increased 3mm and the rest of the director 4, 5 and 6 increased 1mm each.

Table 4.5: Increased width comparison based on S11

Elements	Width, W (mm)			
	Initial	S11(10)	S11 (22)	S11(199)
Reflector, W_R	102	102	102	105
Driven Element, W_E	64	64	68	65
Director 1, W_{D1}	56	56	56	57
Director 2, W_{D2}	40	40	40	41
Director 3, W_{D3}	40	44	40	43

Director 4, W_{D4}	39	39	39	40
Director 5, W_{D5}	39	39	39	40
Director 6, W_{D6}	38	38	38	40

Based on the observation made, when increasing the width of the directors especially Director 3, W_{D3}, positive outcome can be seen in the S-parameter plot where the signal resonated the nearest to the desired frequency with good return loss which is an improvement as compared to S11(initial). However, when the width of the Driven Elements, W_E, is increased, the antenna performance decreased especially when the width margin of the reflector and the driven element reduced. As shown in the result, when the reflector and driven element has the width 102mm and 68mm each respectively for S11(22), the signal resonated at 2.0036GHz while when the reflector and driven element has the width of 105mm and 65mm each respectively, the signal only shifted to the left from S11(10) resonating at 2.3348GHz. Table 4.6 below shows the return loss measurement of all four S11 including the S11 of the initial design.

It can be concluded that, the width of the driven element and the width margin between the reflector and the driven element are the most crucial element in the design in order to achieve the desired outcome.

Table 4.6: S11 measurements in CST Studio Suite

S-Parameter	Frequency (GHz)	Return-Loss (dB)
S1.1 (Initial)	2.1008	-23.3314
	2.3228	-13.3515
S1.1 (10)	2.0936	-16.9639
	2.3348	-17.1052
S1.1 (22)	2.0036	-13.0593
	2.2676	-4.2888
S1.1 (199)	2.0660	-18.2757
	2.2892	-15.0229

4.2.2.1.2 Radiation Pattern at 2.6GHz

Figure 4.7 below shows the radiation pattern of the antenna at 2.6GHz on E-Plane (Phi=90) where the radiation pattern is similar to the initial radiation pattern but slightly wider.
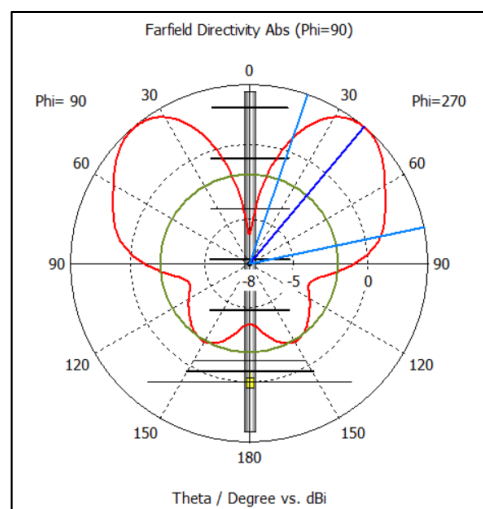
Figure 4.7: Radiation Pattern at 2.6GHz in Polar plot

Figure 4.8 below shows the radiation pattern of the antenna at 2.6GHz in 3D. As depicted in figures (e) and (f), representing the right and left views of the radiation pattern, it is evident that the pattern exhibits the bidirectional radiation pattern. Consequently, the intended outcome was not successfully attained.
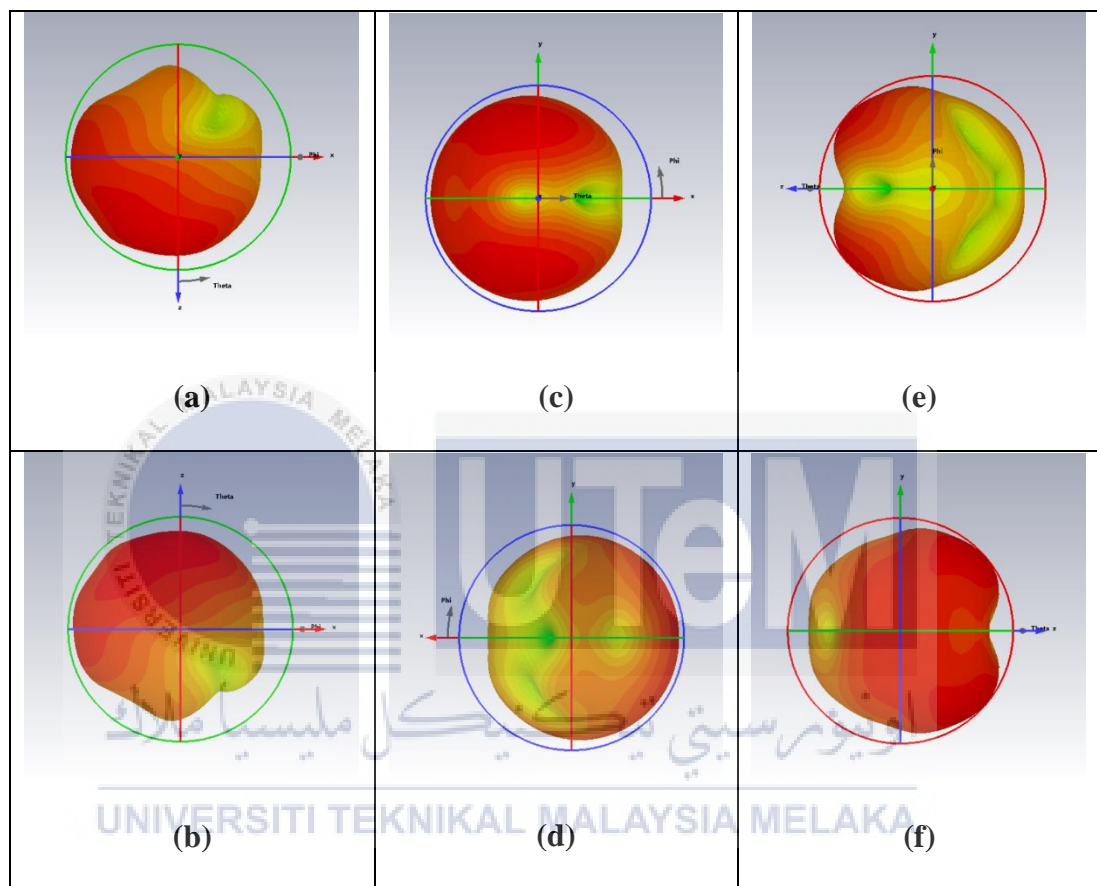
Figure 4.8: 3D Radiation Pattern Overview at 2.6GHz (a)Top-view, (b)Bottom-view, (c)Front-view, (d)Back-view, (e)Right-view, and (f)Left-view

4.2.2.2 Gain, Directivity, Half Power Beamwidth, and Efficiency

Table 4.7 below shows the antenna parameters measurement reading at 2.6GHz after the width increment analysis was done in the parameter sweep. The gain and the directivity deteriorate from 4.278dBi to 3.904dBi for gain and from 4.392dBi to 3.990dBi. The HPBW increased 0.6° and efficiency decreased 0.28% from the initial.

Table 4.7: Antenna parameters measurement

Gain	Directivity	HPBW	Efficiency (Total)
3.904dBi	3.990dBi	59.2°	14.46%

4.2.2.3 Reduced Elements Width Design

The width of the elements was gradually reduced to reach 4mm. To understand how this change affected the antenna, a parameter sweep was conducted using CST Studio Suite. Sequences and parameters were defined in the Time Domain Solver, assigning each parameter to a different sequence. In this case, the parameters included the width of individual coaxial elements, such as the reflector, driven element, and six directors. This process resulted in eight sequences in total. The outcomes of the parameter sweep were then compared to assess the impact of the width increment on the antenna design.

4.2.2.3.1 Reduced Elements Width Return Loss Analysis

Figure 4.9 below shows the comparison of the S11 plotted. In this analysis, a comparison was made among three designs that yielded the most significant outcomes, presented in a single graph. The S11 of the initial design was also incorporated into the plot to observe any potential improvements. In the graphical representation, the S11 of the initial design was represented by a red dash-dot line. S11(1) depicted by a solid green line was chosen as the width of each element has a width reduction where it resonates at 2.3228GHz which is not much different from the initial design. As shown in the figure, S11 and S11(1) are overlapping. S11(11) depicted by a blue solid line was chosen due to the signal resonated nearest to the desired frequency at 2.4416GHz. Lastly, S11(5) depicted by a solid orange line due to the signal resonated

farthest from the desired frequency at 2.1452GHz. All S11 have good return loss below -10dB.
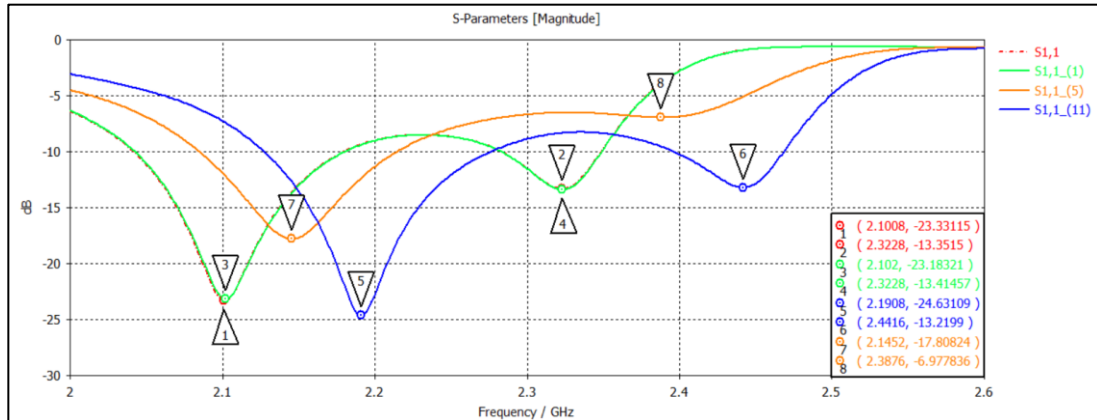
Figure 4.9: Decreased width return-loss analysis

Table 4.8 shows the width changes as compared to the initial elements width where each element width has reduced. According to the table, S11(1) experienced a reduction in the width of each coaxial element, with a decrease of 3mm for each element except for director 6, which only reduced by 1mm. This linear width reduction resulted in the return loss not deviating significantly from the initial result. In the case of S11(11), the element widths were similar to S11, except for Director 3, where the width reduced only by 1mm from the initial width. This resulted in the signal resonating closest to the desired frequency at 2.4416GHz. Meanwhile, S11(5) had similar element widths to S11, except for the driven element, which experienced a width reduction of 1mm. This caused the signal to resonate further from the desired result at 2.1452GHz.

Based on the observation, it was observed that when reducing the width of the director, especially Director 3, to its minimum reduction of 1mm, the optimal outcome was achieved, with the signal resonating closest to the desired frequency of 2.6GHz and a good return loss of -13.2199dB. However, when reducing the width of the driven

element to its minimum reduction of 1mm, along with a decreased width margin between the reflector and the driven element, the antenna resonated further from 2.6GHz at 2.1452GHz, despite maintaining a good return loss at -17.8082dB. The measurement is as shown in Table 4.9.

Table 4.8: Reduced width comparison based on S11

Elements	Width, W (mm)			
	Initial	S11(1)	S11 (11)	S11(5)
Reflector, W_R	102	99	99	99
Driven Element, W_E	64	61	61	63
Director 1, W_{D1}	56	53	53	53
Director 2, W_{D2}	40	37	37	37
Director 3, W_{D3}	40	37	39	37
Director 4, W_{D4}	39	36	36	36
Director 5, W_{D5}	39	36	36	36
Director 6, W_{D6}	38	35	35	35

Table 4.9: S11 measurements in CST Studio Suite

S-Parameter	Frequency (GHz)	Return-Loss (dB)
S11 (Initial)	2.1008	-23.3312
	2.3228	-13.3515
S11 (1)	2.1020	-23.1832
	2.3228	-13.4146
S11 (11)	2.1908	-24.6312
	2.4416	-13.2199
S11 (5)	2.1452	-17.8082
	2.3876	-6.7784

In conclusion, it can be deduced that the width of the driven element and the width margin between the reflector and the driven element are pivotal factors in the design, significantly influencing the antenna's performance and its ability to achieve the desired outcomes.

4.2.2.3.2 Radiation Pattern at 2.6GHz in 1D

Figure 4.10 below shows he radiation pattern of the antenna at 2.6GHz on E-Plane (Phi=90) where the radiation pattern is similar to the initial radiation pattern but narrower with significant main lobe.
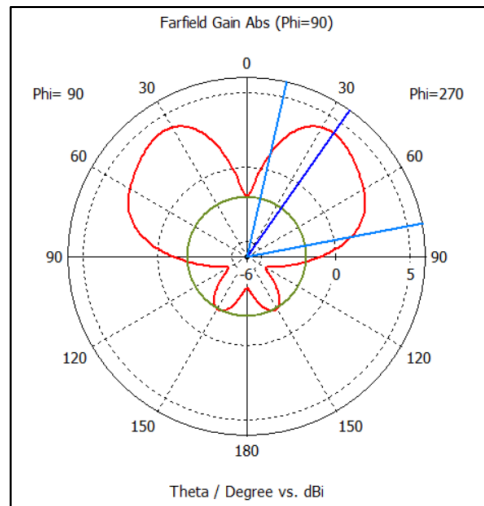
Figure 4.10: Radiation Pattern at 2.6GHz in Polar Plot

Figure 4.11 below shows the radiation pattern of the antenna at 2.6GHz in 3D. The right view and the left view of the radiation shows a slightly wider apple-like radiation pattern with the rest of the view shows and omnidirectional radiation pattern. The radiation pattern is not unidirectional as desired.

(a)	**(b)**	**(e)**
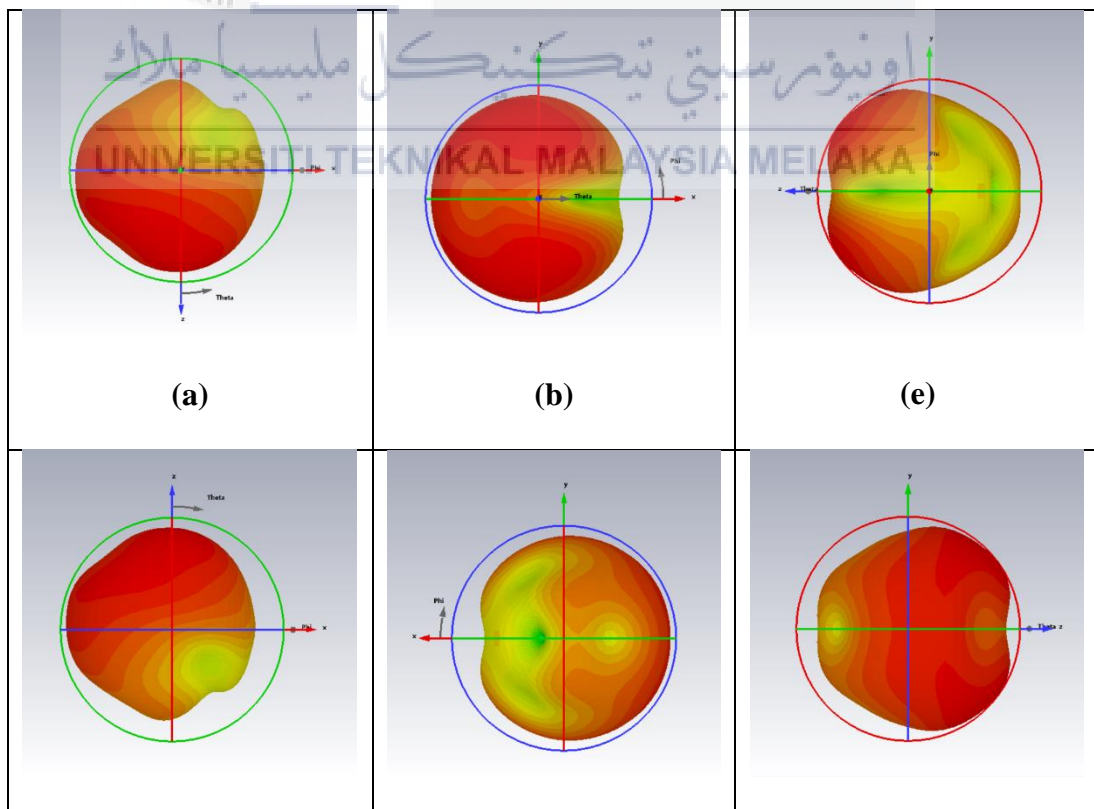
(b)	(d)	(f)

Figure 4.11: 3D Radiation Pattern Overview at 2.6GHz (a)Top-view, (b)Bottom-view, (c)Front-view, (d)Back-view, (e)Right-view, and (f)Left-view

4.2.2.4 Gain, Directivity, Half Power Beamwidth, and Efficiency

Table 4.10 below shows the antenna parameters measurement reading at 2.6GHz after the width reduction analysis was done in the parameter sweep. The gain and the directivity have a slight decrement from 4.278dBi to 4.104dBi for gain and from 4.392dBi to 4.193dBi. The HPBW increased 7.7° and efficiency increased 2.11% from the initial.

Table 4.10: Antenna parameters measurement

Gain	Directivity	HPBW	Efficiency (Total)
4.104dBi	4.193dBi	66.3°	16.85%

4.2.2.5 Comparison between Increased Width and Decreased Width Design

Figure 4.12 below shows the comparison between the most significant result from increasing the elements width and reducing the elements width. For the increased element width design, S11(10) was chosen and for the reduced element width design, S11(11) was chosen both for the same reason, resonating at the frequency nearest to desired frequency of 2.6GHz. as shown in the figure, S11(11) is resonated nearest to 2.6GHz at 2.4416GHz compared to S11(10) at 2.3348GHz. This shows that by reducing the width of the elements will lead to main goal of having the signal resonate at 2.6GHz with a good return loss below -10dB.
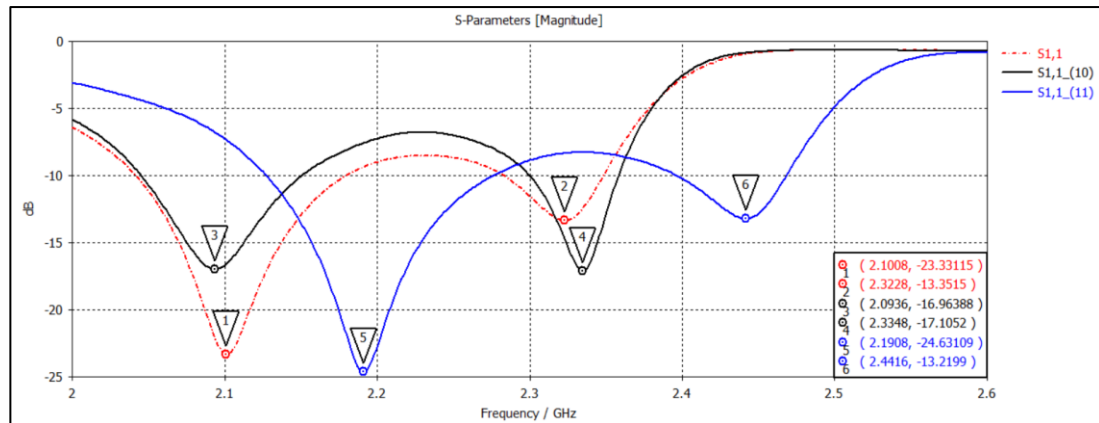
Figure 4.12: S11 comparison between increased width design and decreased width design

Table 4.11 below shows the return loss at each frequency resonated for three designs: initial design, increased width design and reduced width design.

Table 4.11: S11 comparison between increased width design and decreased width design

Design	S-Parameter	Frequency (GHz)	Return-Loss (dB)
Initial	S11 (Initial)	2.1008	-23.3312
		2.3228	-13.3515
Increased Width	S11 (10)	2.0936	-16.9639
		2.3348	-17.1052
Reduced Width	S11 (11)	2.1908	-24.6312
		2.4416	-13.2199

In term of antenna performance, Table 4.12 below shows the parameters comparison between increased width design and reduced width design. As shown in the table, reducing the elements width has better gain and directivity with difference 0.2dBi for gain and 0.203dBi for directivity. In addition, the reduced width design has

higher efficiency at 16.85% which is 2.39% higher than the increased-width design.

By reducing the size of the antenna elements the gain is increased [13].

Table 4.12: Parameters comparison between increased width design and reduced width design

	Gain	Directivity	HPBW	Efficiency (Total)
Increased Width	3.904dBi	3.990dBi	59.2°	14.46%
Reduced Width	4.104dBi	4.193dBi	66.3°	16.85%

4.2.3 Proposed Yagi Antenna Design

Following the analysis of antenna width, the design optimization phase focuses on refining and enhancing the Yagi-Uda antenna to achieve optimal performance. This process involves leveraging insights gained from the width analysis to make strategic adjustments to the antenna's configuration, dimensions, and other relevant parameters. The primary goals of design optimization are to maximize key performance metrics such as gain, directivity, and efficiency while ensuring compatibility with the frequency band 2.6GHz.

4.2.3.1 Antenna Design

Figure 4.13 below shows the proposed design overview of the rectangular-disk Yagi-Uda antenna using CST Studio Suite. The figures show the front-view, back-view and the perspective-view of the initial antenna design.
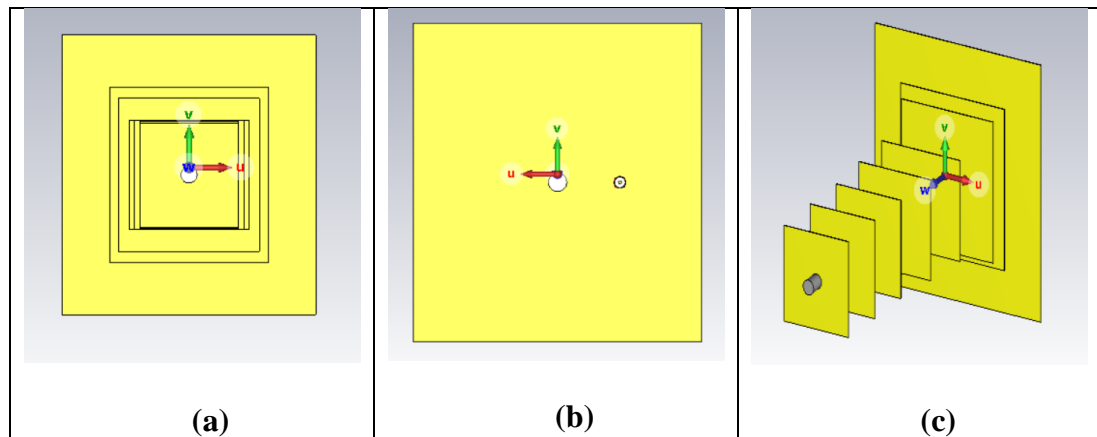
Figure 4.13: Optimized design overview (a)front-view, (b)back-view and (c)perspective-view

The dimension of the optimized Ygi-Uda antenna is as shown in Table 4.13. in this design, the elements width were reduced except for Director 2 and 3. From the analysis, it was observed that when the directors width especially Director 3 were increased, the S11 plotting shows good return loss.

Table 4.13: Elements dimension of the optimized design

Components	Dimension (mm)			
	Width, W		Length, L	
Reflector	W_R	92.48	L_R	102
Driven Element	W_E	57.99	L_E	64
Director 1	W_{D1}	51.29	L_{D1}	56
Director 2	W_{D2}	43.84	L_{D2}	40
Director 3	W_{D3}	40.21	L_{D3}	40
Director 4	W_{D4}	36	L_{D4}	39
Director 5	W_{D5}	36	L_{D5}	39
Director 6	W_{D6}	36	L_{D6}	38

Figure 4.14 and Table 4.14 show the distance between the elements of the antenna. The distance between the coaxial elements were set uniformly to maintain the antenna stability. The spacing affects various parameters such as the impedance matching, radiation pattern, and overall efficiency of the antenna. A consistent and well-defined spacing helps in achieving a balanced distribution of electromagnetic fields between the driven element, directors, and reflector, which contributes to the desired directional characteristics of the Yagi-Uda antenna. As shown in the table, the distance between the reflector and the driven element and the distance between the driven element and the Director 1 were set at 5mm while the distance between the directors were set at 25mm, same as the initial design.
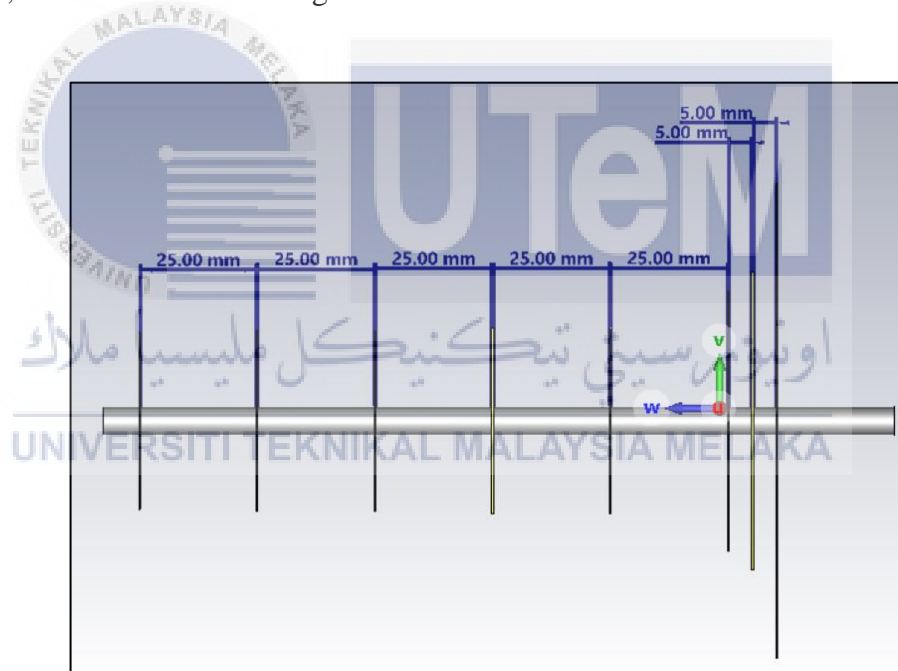
Figure 4.14: Distance between elements

Table 4.14: Distance between elements

Elements	Distance (mm)
Reflector to Driven Element, $S_{ref-dri}$	5
Driven Element to Director 1, $S_{dri-dir1}$	5
Director 1 to Director 2, $S_{dir1-dir2}$	25
Director 2 to Director 3, $S_{dir2-dir3}$	25
Director 3 to Director 4, $S_{dir3-dir4}$	25
Director 5 to Director 6, $S_{dir5-dir6}$	25

4.2.3.2 S-Parameter

The simulated return loss (S11) result is shown in Figure 4.15. It is clear that the proposed antenna exhibited a stopband response at 2.236GHz - 2.460GHz and 2.586GHz - 2.613GHz with the return loss almost below -10dB. As for the return loss, the antenna resonates at 2.384GHz with excellent return loss at -30.1816dB and at 2.6GHz with return loss of -15.0241dB which is good as shown in Table 4.15. The desired return loss is achieved.
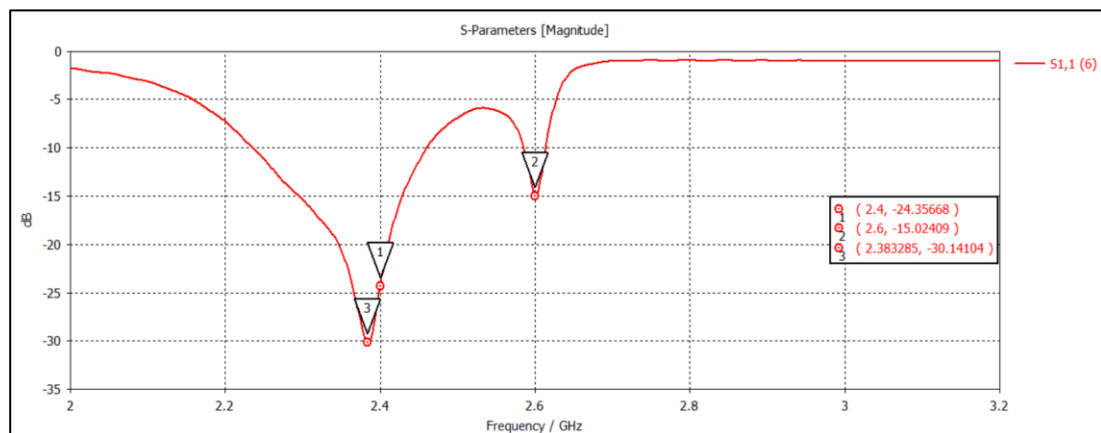
Figure 4.15: Simulated S11 of the optimized design

Table 4.15: Return-loss measurement of the optimized design

Frequency (GHz)	Return-Loss (dB)
2.38	-30.1410
2.60	-15.0241

4.2.3.3 Radiation Pattern

The following parameter measured the antenna radiation pattern for the frequency 2.38GHz and 2.6GHz as shown in Figure 4.16 and Figure 4.17 respectively. Radiation pattern for all antenna were measured at *Phi=90* degrees (E-Field). As shown in the figure, both radiation pattern are unidirectional radiation pattern however, at the frequency 2.384GHz, the radiation pattern is narrower and the main lobe is longer compared to the radiation pattern at the frequency 2.6GHz showing that the performance of the antenna is slightly better at 2.384GHz than at 2.6GHz.

Figure 4.16: Radiation Pattern in Polar plot for the frequency 2.38GHz

Figure 4.17: Radiation Pattern in Polar plot for the frequency 2.6GHz
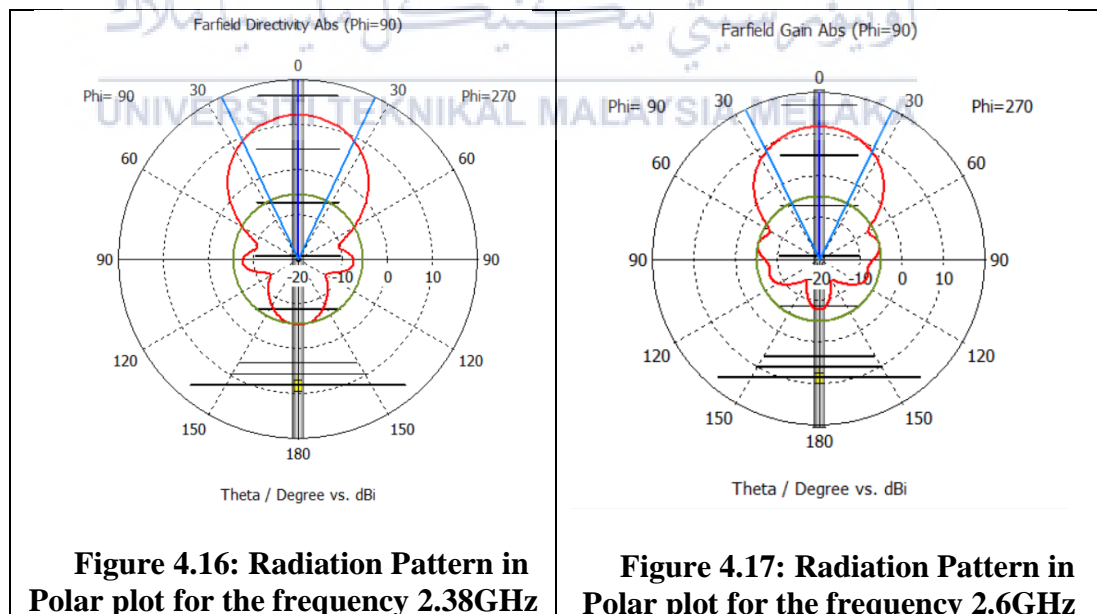
Figure 4.18 below shows the radiation pattern of the optimized antenna at 2.384GHz in 3D from various angle.

(a)	**(c)**	**(e)**
(b)	**(d)**	**(f)**
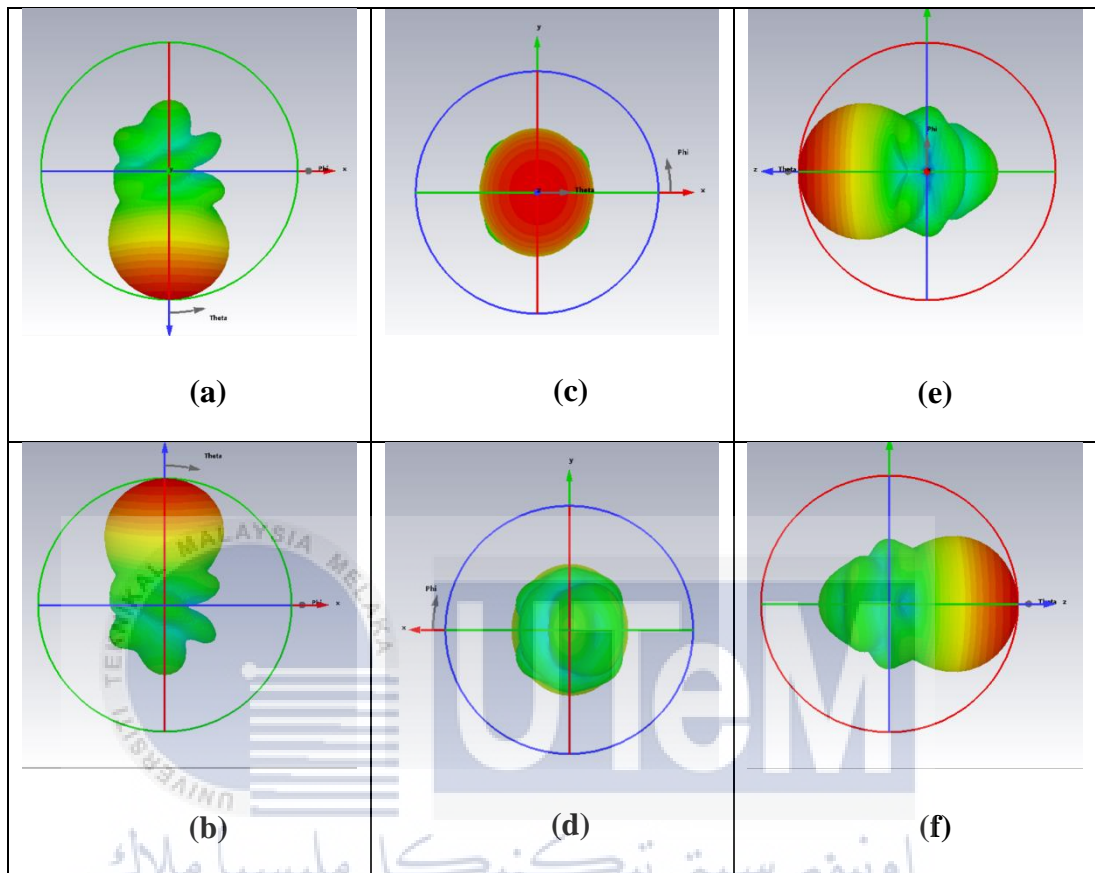
Figure 4.18: 3D Radiation Pattern Overview at 2.3GHz (a)Top-view, (b)Bottom-view, (c)Front-view, (d)Back-view, (e)Right-view, and (f)Left-view

Figure 4.19 below shows the radiation pattern of the optimized antenna at 2.6GHz in 3D from various angle. The radiation pattern is slightly wider and the main lobe is slightly shorter than the radiation pattern at 2.384GHz.
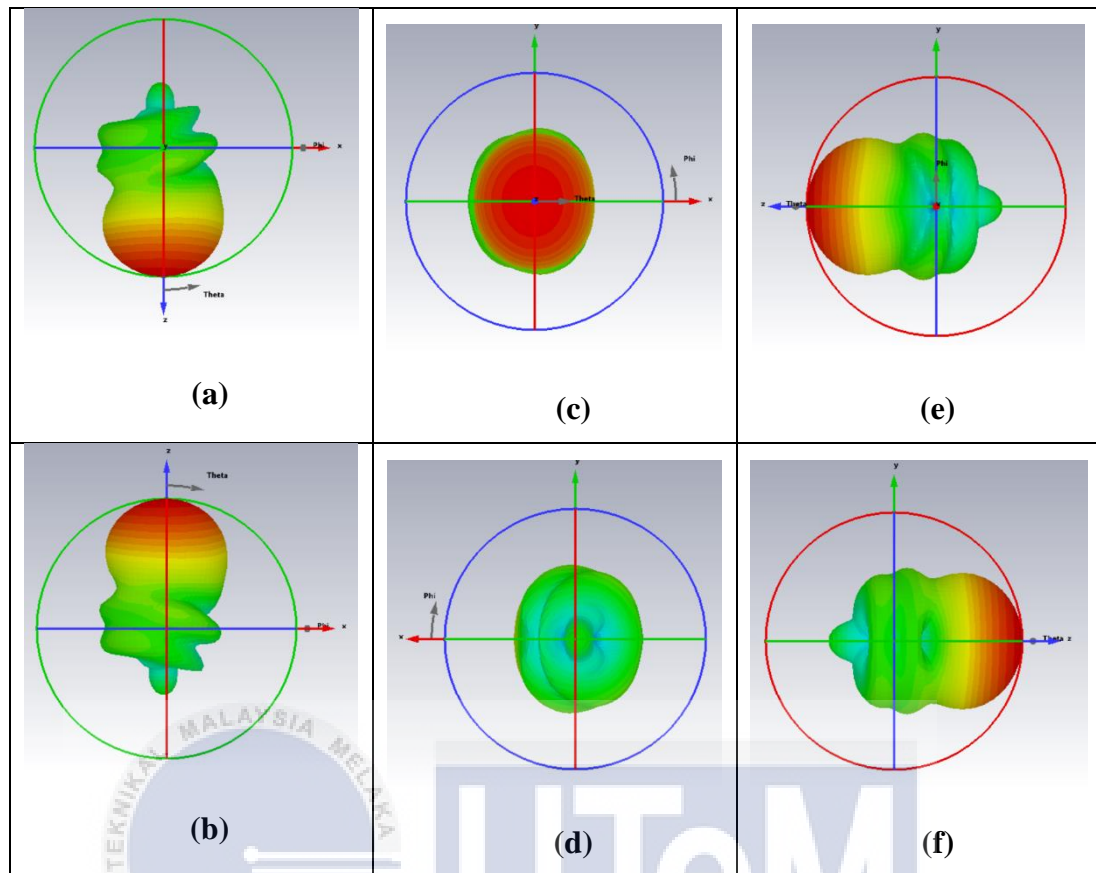
Figure 4.19: 3D Radiation Pattern Overview at 2.6GHz (a)Top-view, (b)Bottom-view, (c)Front-view, (d)Back-view, (e)Right-view, and (f)Left-view

4.2.3.4 Gain, Directivity, Half Power Beamwidth, and Efficiency

The gain, directivity, HPBW and efficiency of the antenna with optimal dimensions can be viewed through the radiation pattern in 3D polar graph in Figure 4.19 and Table 4.16. It can be stated that the antenna's overall performance is slightly superior at 2.384GHz compared to 2.6GHz. The radiation pattern at 2.384GHz exhibits a narrower profile, resulting in a correspondingly narrower Half Power Beamwidth (HPBW) compared to 2.6GHz. Nevertheless, the overall performance at 2.6GHz remains excellent.

In summary, the optimized outcomes align with the desired specifications, showcasing resonance at the frequency of 2.6GHz with high gain and directivity exceeding 10dBi, coupled with an efficiency surpassing 90%.

Table 4.16: Antenna parameters measurement at 2.3GHz and 2.6GHz

Frequency	Gain	Directivity	HPBW	Efficiency
2.384GHz	12.07 dBi	12.09 dBi	45.3°	99.31%
2.6GHz	11.74 dBi	11.85 dBi	52.4°	94.51%

4.3   4G LTE Yagi-Uda Antenna Development

Figure 4.20 below shows the developed rectangular-disk Yagi-Uda antenna for 4G LTE coverage enhancement system ready to be tested. The antenna elements were made of recycled biscuit can that was attached to the threaded metal rod. SMA feeder were soldered to the reflector and the pin was soldered to the driven element. The directors and reflectors are commonly referred to as parasitic elements since they are not directly fed with the signal [36].
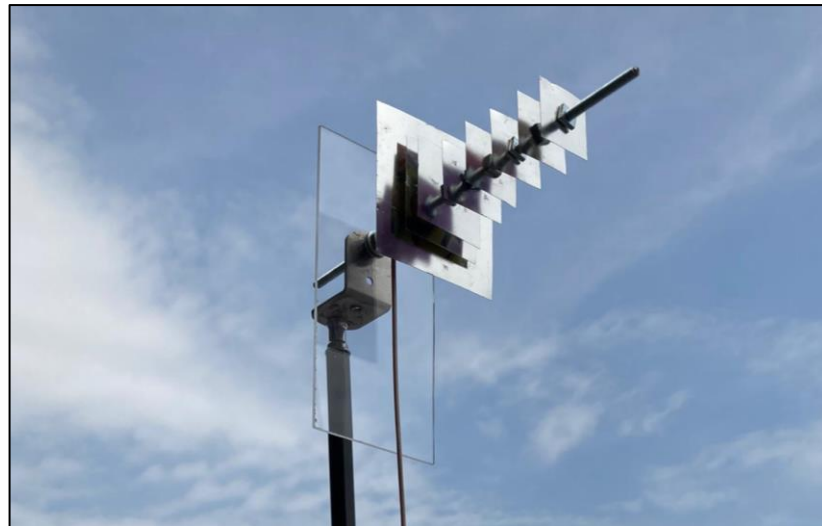
**Figure 4.20: Developed Yagi-Uda Antenna for 4G LTE Coverage
Enhancement System**

Table 4.17 below shows the dimension used to develop the antenna coaxial
elements. The dimensions employed for constructing the antenna were derived from
the optimized antenna design in CST Studio Suite, ensuring the antenna achieves its
highest gain, directivity, and efficiency.

Table 4.17: Elements Dimension

Components	Dimension (mm)			
	Width, W		Length, L	
Reflector	W_R	92.48	L_R	102
Driven Element	W_E	57.99	L_E	64
Director 1	W_{D1}	51.29	L_{D1}	56
Director 2	W_{D2}	43.84	L_{D2}	40
Director 3	W_{D3}	40.21	L_{D3}	40
Director 4	W_{D4}	36	L_{D4}	39

| Director 5 | W_{D5} | 36 | L_{D5} | 39 |
| Director 6 | W_{D6} | 36 | L_{D6} | 38 |

Table 4.18 below shows the distance between elements of the developed antenna. Initially, the distance between Driven Element and Director 1, $S_{dri-dir1}$ was 5mm and the distance between director to director was 25mm, similar to the simulation design. However, as the antenna was tested using PNA-X Network Analyzer for S11 measurement, the signal resonated at 2.3GHz which was not as desired. Then, the distance between elements were tuned until the signal resonated at 2.6GHz or within the frequency band of Band 7, 2.51GHz to 2.64GHz for Maxis Broadband Sdn. Bhd. telco [37] as allocated by Malaysia Communications and Multimedia Commissions (MCMC). The tuning method is called parameter tuning or optimization [36].

Table 4.18: Distance between elements

Elements	Distance (mm)
Reflector to Driven Element, $S_{ref-dri}$	5
Driven Element to Director 1, $S_{dri-dir1}$	7
Director 1 to Director 2, $S_{dir1-dir2}$	18
Director 2 to Director 3, $S_{dir2-dir3}$	18
Director 3 to Director 4, $S_{dir3-dir4}$	19
Director 5 to Director 6, $S_{dir5-dir6}$	18

4.4   Lab Test Measurement

Following the development of the 4G LTE antenna, laboratory testing of the antenna was undertaken. Initially, the return loss of the antenna was measured using

the PNA-X Network Analyzer. Subsequently, the antenna was placed within the anechoic chamber to evaluate its functionality in the transceiver system, obtaining measurements for gain and radiation pattern.

4.4.1   S-Parameter

Figure 4.21 below shows the finalized return-loss measurement of the proposed antenna. The antenna signals resonate at 2.374 GHz and 2.589GHz which are within the range for Band 40 frequency spectrum range at 2.3GHz to 2.4GHz [38] and Band 7 frequency spectrum range at 2.51GHz to 2.64GHz for Maxis Broadband Sdn Bhd telco [37]. However, for the 2.3GHz frequency spectrum, it is only limited to UniFi, a wireless mobile service arm by Telekom Malaysia Berhad [38]. It is a licensed 4G LTE frequency band.
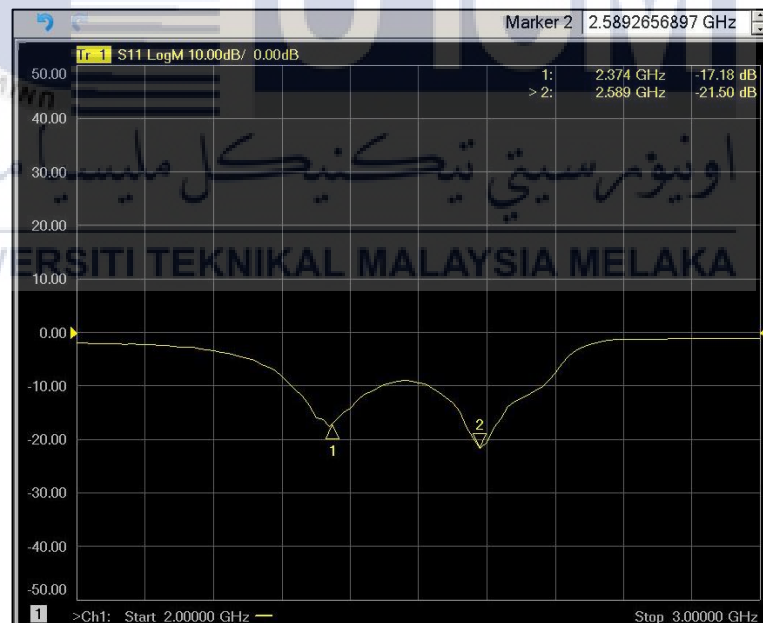
Figure 4.21: Measured S11

Table 4.19 below shows the return loss at the resonant frequencies was measured, with the S11 measurement registering at -17.18dB for 2.374GHz and -21.50dB for 2.589GHz. At both frequencies, the return loss exhibited favorable values, being below -10dB **[12]**.

Table 4.19: Return-loss measurement of the developed antenna

Frequency (GHz)	S11 (dB)
2.374	-17.18
2.589	-21.50

4.4.2   Radiation pattern

Figure 4.22 and Figure 4.23 below show the radiation pattern obtained for 2.374GHz and 2.6GHz observed in *E*-plane respectively. The radiation patterns for both frequencies exhibited a unidirectional nature, with main lobe magnitudes of 10.527 dB and 9.950 dB, respectively. The findings indicate that the main lobe magnitude at 2.4GHz surpassed that at 2.6GHz, signifying a stronger resonance of the signal at 2.4GHz compared to 2.6GHz as shown in Table 4.19. Consequently, it is apparent that the radiation pattern preserves its characteristics and form, closely resembling the simulated pattern, as indicated in [14]. Hence, there is minimal variation between the measured and simulated radiation of the antenna. Parameters like the main lobe and back lobe also align closely with the simulated positions.
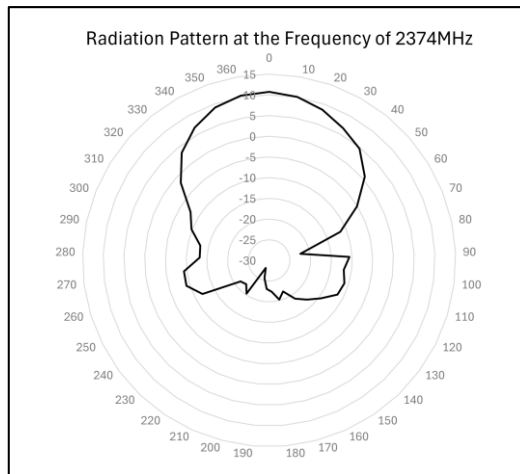
Figure 4.22: Radiation Pattern at the frequency of 2.4GHz
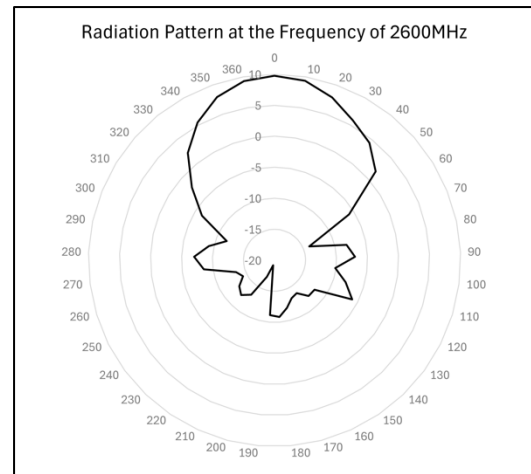
Figure 4.23: Radiation Pattern at the frequency of 2.6GHz

4.4.3 Gain, Directivity, Half Power Beamwidth (HPBW) and Efficiency

Table 4.20 below shows the antenna parameters measurement measured at both frequency 2.4GHz and 2.6GHz. The proposed antenna exhibits high forward gain and directivity at both frequencies. The gain is noteworthy, exceeding 10dB at 2.4GHz and nearing 10dB at 2.6GHz, specifically at 9.950dB with a minimal difference. Moreover, both frequencies demonstrate commendable antenna efficiency, surpassing 67%. It's worth noting that practical antennas typically fall within the 50% to 70% efficiency range due to diverse factors, including design, materials, operating frequency, and environmental conditions. In terms of directivity, both frequencies showcase elevated values, surpassing 10dB.

Table 4.20: Antenna parameters measurement at 2.3GHz and 2.6GHz

Frequency	Gain	Directivity	HPBW	Efficiency
2.374GHz	10.812 dB	12.638 dB	51°	67.69%
2.6GHz	9.950 dB	11.686 dB	54°	67.05%

4.5   Comparison between CST Studio Suite Simulation and Lab Test Measurement Result

Table 4.21 compares the performance of the antenna between the simulation antenna and the developed antenna. In term of return loss, the signal resonates more strongly at 2.6GHz, measuring at -21.5dB, compared to the simulation where the signal resonates more effectively at 2.384GHz with a value of -30.1410dB. In terms of gain, both the simulation and measured results for both frequencies demonstrate a high-gain antenna, with a slight difference favoring higher gains in the simulation. Both the simulation and measured outcomes also indicate high directivity, where the measured directivity at 2.38GHz is slightly higher than in the simulation, and at 2.6GHz, the measured directivity is marginally lower than in the simulation. Efficiency, as depicted by both simulation and measurements, is commendable, with the simulation design achieving above 90%. While ideal efficiency in simulation is 100%, practical antennas commonly fall within the 50% - 70% efficiency range due to various influencing factors, which is considered favorable. Therefore, these findings suggest that both the simulation and the developed antenna exhibit strong performance.

Table 4.21: Parameters comparison between simulation and measured

Frequency	2.3GHz (Band 40)		2.6GHz (Band 7)	
	Simulation	Measured	Simulation	Measured
Return loss	-30.141 dB	-17.180 dB	-15.024 dB	-21.500 dB
Gain	12.070 dB	10.812 dB	11.740 dB	9.950 dB
Directivity	12.090 dB	12.638 dB	11.850 dB	11.686 dB
Efficiency	99.31%	67.69%	94.51%	67.05%

HPBW	45.3°	51°	52.4°	54°

4.6 Field Test Measurement

Field testing was conducted after the antenna desired return loss, gain, directivity and radiation pattern were obtained. This test was held to test the antenna performance in real-life transceiver system.

4.6.1 Field Test Location

The field test was conducted at Taman Bukit Tambun Perdana 2, Durian Tunggal, Melaka and the base station used to communicate with the Yagi-Uda antenna is located next to the North-South Expressway Southern Route. Figure 4.24 below shows the base station location with the tower information using Cellmapper.net.
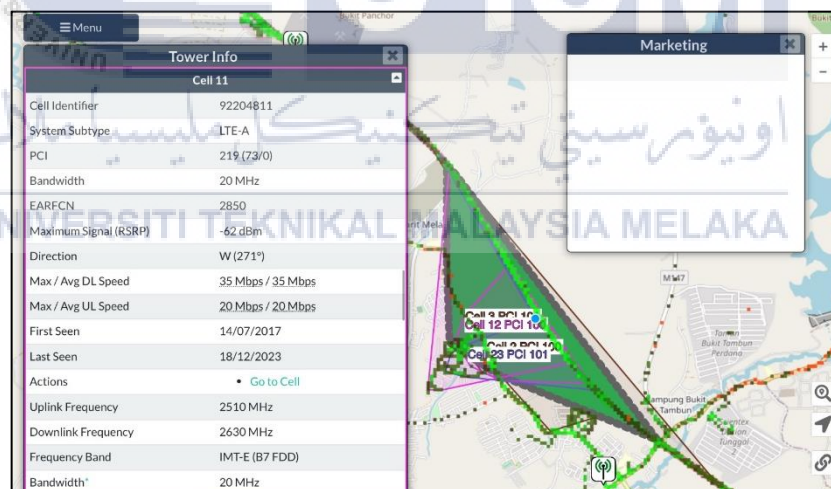
Figure 4.24: Base station location in Cellmapper.net

Figure 4.25: Base tower.

The base station supports three 4G LTE frequency bands: Band 3 (1.8GHz), Band 7 (2.6GHz), and Band 8 (900MHz). Specifically, for the Band 7 (2.6GHz) frequency band, communication with the Yagi-Uda Antenna was established through Cell 11. This particular cell covers the designated field-test area.

The 4G LTE Yagi-Uda antenna was set up facing towards the base station direction with high directivity and gain in order to obtain the best antenna performance. This is due to Yagi-Uda antenna is a unidirectional antenna where its performance is dependent on the antenna directivity. The distance between the field test area and the location of the base station that communicate with the Yagi-Uda antenna is as shown in Figure 4.26 at 2421.36 m.
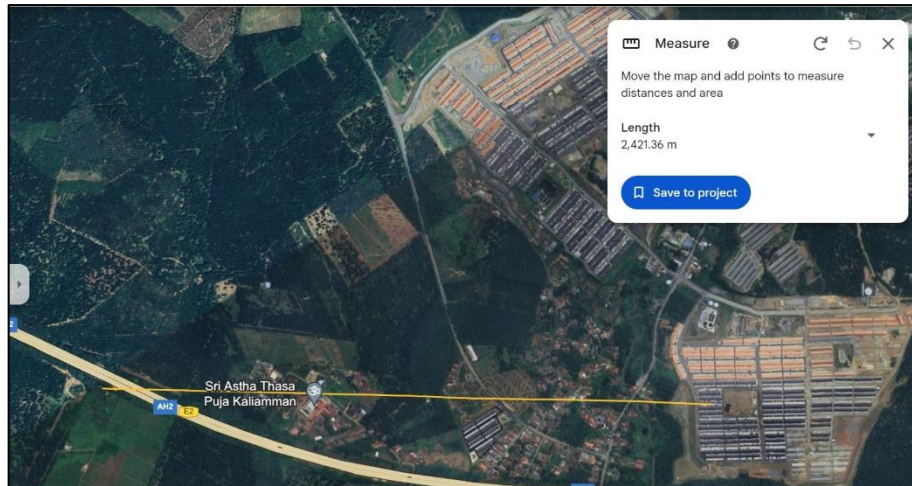
Figure 4.26: Distance between field-test area and base station.

4.6.2 4G LTE Signal Strength Performance

Further exploration of the 4G network's performance is necessary to enhance its utilization and ensure user satisfaction. The 4G LTE signal strength must be put into test to observe the functionality and signal performance of the developed antenna. The quality parameters under examination include Reference Signal Received Power (RSRP), Reference Signal Received Quality (RSRQ), and Signal to Noise Ratio (SNR) [39].

RSRP represents the received signal power in decibels (dBm) at the User Equipment (EU). The RSRP value decreases as the distance between the site and the EU increases and vice versa. RSRQ measures the quality of the signal received by the EU in decibels (dB) from a cell. It is calculated as the ratio of the number of RSRP resource blocks to the Received Signal Strength Indicator (RSSI). RSRQ is impacted by signals, noise, and interference encountered by the EU. SINR, on the other hand, is the ratio of received signal power to the interference power and noise power experienced by the user. While SINR is a parameter indicating signal quality, it serves

as a reference for overall network quality [40]. The standard range of the performance indicator can be referred to Appendix G.

4.6.2.1 4G LTE Signal Strength Performance with Buit-in Antenna

The built-in antenna refers to the antenna housed within the 4G LTE router, which usually broadcasts signals in all directions. Configuring the router's antenna settings via the router's IP address enables the router to utilize this internal antenna for signal broadcasting without the need for an external antenna. Table 4.22 below shows the signal performance of the router with the built-in antenna. For the signal strength, RSRP obtained was between -110dBm to -100dBm which is categorized as poor or weak while RSRQ falls between -17dBm to -14dBm which is also categorized as fair or middle. The SINR falls between -20dBm to -3dBm which is categorized as very poor. The signal strength does not meet the criteria of a good signal strength, therefore, the upload and download speed are slow at 5.86Mbps and 9.47Mbps.

Table 4.22: Signal performance with Built-in Antenna

Category	Elements	Measurement	Evaluation	Percentage
Signal Strength	RSSI	-68 dBm	Very Good	76%
	RF – Margin	-35 dBm	Bad	1%
	RSRP	-104 dBm	Weak	28%
	RSRQ	-15 dBm	Middle	51%
	SINR	-4 dBm	Bad	25%
Speed	Upload	5.86 Mbps	-	-
	Download	9.47 Mbps	-	-

4.6.2.2 4G LTE Signal Strength Performance with 4G LTE Yagi-Uda Antenna

Configuring the router's antenna settings via the router's IP address enables the router to utilize the proposed antenna for signal broadcasting as an external antenna. Table 4.23 below shows the signal performance of the router with the proposed antenna. For the signal strength, RSRP obtained was between -90dBm to -80dBm which is categorized as good or middle while RSRQ falls between -10dBm to -3dBm which is also categorized as good. The SINR falls between 0dBm to 3dBm which is categorized as fair. The signal strength does meet the criteria of a good signal strength, therefore, the upload and download speed are better at 14.1Mbps and 20.2Mbps respectively.

Table 4.23: Signal performance with 4G LTE Yagi-Uda Antenna

	Elements	Measurement	Evaluation	Percentage
	RSSI	-65 dBm	Very Good	81%
	RF – Margin	-24 dBM	Excellent	100%
Signal Strength	RSRP	-89 dBm	Middle	48%
	RSRQ	-7 dBm	Good	77%
	SINR	1 dB	Bad	36%
Speed	Upload	14.1 Mbps	-	-
	Download	20.2 Mbps	-	-

4.6.2.3 Comparison of the Internet Connection Performance Before and After Implementing the 4G LTE Yagi-Uda Antenna.

Table 4.24 presents three key parameters used to assess the RF connectivity status of the network: RSRP, RSRQ, and SINR. Among these parameters, SINR (Signal-to-

Interference and Noise Ratio) is identified as the most critical, as it determines the signal quality in a 4G LTE network. SINR requires a minimum of -20dB to detect RSRP and RSRQ and signifies the throughput capacity of the channel. With the antenna in use, SINR shows an 11% increase compared to when the built-in antenna was utilized, indicating an enhancement in signal strength.

Upon connecting the antenna, there is a substantial 99% increase in the RF Margin compared to the built-in antenna. Moving on to RSRP (Reference Signal Received Power), it represents the strength of LTE Reference Signals spread across the entire bandwidth. A good RSRP alone does not define data rates; it is SINR that significantly impacts connection speeds. Results from Table 4.24 show that without the antenna, RSRP is below -100dB, but with the antenna, it surpasses -100 dBm, marking an improvement from weak to middle signal strength, a notable 20% increment.

The third parameter, RSRQ (Reference Signal Received Quality), measures Carrier-to-Interference (C/I) and indicates the quality of the reference signal. The RSRQ received with the antenna improves from -15dB to -7dB, resulting in a 26% overall enhancement, signifying better network reception quality in the presence of the proposed antenna.

In summary, the network signal for Maxis telco is considerably improved with the antenna, as indicated by the Received Signal Strength Indication (RSSI) within the range of -65dBm to -75dBm, categorized as good, with strong signal strength and good data speed. Placing the antenna outdoors towards the tower's direction enhances SINR, leading to an overall improvement in the network signal for Maxis telco reception to the router. This improvement is substantiated by a significant increase in download speed, up by 10.73Mbps (52.62% increment), and an improvement in upload speed by

8.24Mbps (58.44% increment), validating the boosted network signal with the proposed antenna.

Table 4.24: Signal strength performance comparison between when using Built-in antenna and 4G LTE Yagi-Uda antenna

	Elements	Built-in Antenna	Proposed Antenna	Percentage Increment
Signal Strength	RSSI	-68 dBm	-65 dBm	5%
	RF - Margin	-35 dBm	-24 dBm	99%
	RSRP	-104 dBm	-89 dBm	20%
	RSRQ	-15 dBm	-7 dBm	26%
	SINR	-4 dBm	1 dB	11%
Speed	Upload	5.86 Mbps	14.1 Mbps	58.44%
	Download	9.47 Mbps	20.2 Mbps	52.62%

4.7 Environment and Sustainability

In the evolving landscape of the COVID-19 pandemic, reliable internet connectivity has evolved into a critical necessity for various aspects of daily life, spanning education, business, healthcare, and communication. Despite this, certain regions, especially rural areas, continue to grapple with insufficient internet access. The development of an environmentally sustainable Yagi antenna emerges as a potential solution to enhance 4G LTE mobile applications in homes, schools, offices, and similar establishments situated in these underserved rural areas.

Collaborative efforts with educational institutions or universities could facilitate the installation of these Yagi antennas in schools within rural regions. This approach not

only addresses the challenge of limited internet connectivity but also presents an opportunity to enrich student learning experiences through hands-on experimental classes. Beyond improving internet access, the initiative aims to expose students to the practical applications of antenna and microwave studies in real-world scenarios.

Since the project is successfully implemented, this project aligns with the broader goals of Sustainable Development Goal (SDG) 4, which seeks to ensure equitable and inclusive quality education, offering possibilities for lifelong learning for individuals across various demographics [41]. This match the SDG 4 Target 4.4 where they aim by the year 2030, significantly enhance the quantity of young individuals and adults possessing pertinent skills, encompassing technical, vocational skills, fostering employment, decent job opportunities, and entrepreneurial pursuits [41] [42].

Taking a sustainable and cost-effective approach, the Yagi-disk antenna involves repurposing conductive materials sourced from biscuit tins to create the disk component of the Yagi antenna. This aligns with SDG Goal 12, which focuses on responsible consumption and production. The utilization of tin waste in this manner contributes to reducing the demand for new raw materials, minimizing waste sent to landfills, and promoting resource conservation. Additionally, it aids in reducing air and water pollution, lowering greenhouse gas emissions, and fostering sustainable practices in material use and disposal. This match their Target 12.5, By the year 2030, significantly decrease the generation of waste through preventive measures, reduction strategies, recycling, and the promotion of reuse [43] [44].

CHAPTER 5

CONCLUSION AND FUTURE WORKS

5.1 Introduction

This segment will outline the project's conclusion and recommendations. It entails summarizing the project, discussing its findings, and proposing suggestions for potential improvements.

5.2 Conclusion

In conclusion, this project aimed to design and develop a unidirectional Yagi-Uda antenna with the primary objective of enhancing 4G LTE coverage. The achievement of this goal involved a systematic approach and the fulfillment of three specific objectives.

The first objective focused on the design and development of the unidirectional Yagi-Uda antenna. Through the utilization of CST Studio Suite and parameter sweeps, the antenna's dimensions and characteristics were optimized to ensure optimal performance at 2.6GHz. Throughout the project, the antenna managed to cover two 4G LTE band at 2.6GHz (Band 7) and 2.3GHz (Band 40) which make it a unidirectional dual-band rectangular Yagi-Uda antenna. This offers a wider range frequency selection for user and application. The successful completion of this objective lays the foundation for improved 4G LTE coverage, contributing to the enhancement of internet connectivity in various applications.

The second objective centered on analyzing the impact of changes in the width of the antenna elements. Through parameter sweeps in CST Studio Suite, the project systematically assessed how variations in width influenced key antenna parameters such as gain, directivity, and efficiency. The antenna go through three stage of analysis: increasing, reducing and optimizing the elements width to find the optimal dimension with the best antenna performance. This analysis provided valuable insights into the sensitivity of the antenna design to specific dimensional changes, aiding in the refinement of the overall design for better performance.

The third objective involved the evaluation of the antenna's performance in a transceiver system. Lab testing, including measurements of return loss, gain, and radiation pattern, provided crucial data on the real-world functionality of the developed antenna. The comparison between simulation and measured results demonstrated the reliability and effectiveness of the design, validating its practical application in a transceiver system. Field testing, including the measurement of signal

strength and speed to prove the enhancing element of the antenna and the difference it brought comparing to the built-in antenna of the router.

Overall, the project successfully met its objectives, resulting in the creation of a high-performance unidirectional Yagi-Uda antenna optimized for 4G LTE coverage. The systematic analysis of antenna element width variations and the comprehensive evaluation in a transceiver system contribute to the body of knowledge in antenna design and wireless communication. The outcomes of this project have practical implications, especially in addressing connectivity challenges in areas with poor internet access, thus aligning with the broader goals of improving digital connectivity and accessibility.

5.3   Future Work

These extensive future work suggestions aim to advance the project's impact, scalability, and adaptability, positioning the Yagi-Uda antenna as a sustainable and effective solution for improving wireless communication in diverse settings.

1. **Frequency Band Expansion**: The exploration of frequency band expansion involves adapting the Yagi-Uda antenna to encompass a broader spectrum, extending beyond the confines of 4G LTE to include frequencies relevant to 5G and emerging wireless communication technologies. This necessitates a comprehensive study of the antenna's design parameters, such as element lengths and spacings, to accommodate the unique characteristics of different frequency bands. Compatibility with multiple frequency bands is crucial to enhance the antenna's versatility, enabling it to cater to evolving communication standards. It requires an in-depth understanding of the electromagnetic properties of various frequency bands and a careful

adjustment of the antenna's configuration to optimize performance across these bands.

2. **Interference Mitigation Strategies:** In addressing interference challenges, the project aims to investigate a range of strategies to mitigate disruptions caused by other wireless devices or environmental factors. This involves the implementation of advanced filtering techniques or adaptive algorithms designed to enhance signal quality and reduce vulnerability to interference. Filtering mechanisms can be employed to selectively pass desired frequencies while attenuating unwanted signals. Adaptive algorithms may dynamically adjust the antenna's parameters in response to changing interference conditions. The research will delve into the effectiveness of these strategies in real-world scenarios, considering factors such as signal-to-noise ratio and the spectral characteristics of interfering signals.

3. **Integration with 5G Networks:** To ensure the seamless integration of the Yagi-Uda antenna with 5G networks, an exhaustive investigation into the specific requirements of 5G technology is imperative. This includes analyzing the frequency bands designated for 5G communication and understanding the technical specifications unique to 5G networks. Modifications to the Yagi-Uda antenna design may be necessary to align with the characteristics of 5G signals, such as higher frequencies and increased data rates. The integration process will also consider the potential for beamforming and other advanced features associated with 5G technology. This investigation aims to position the Yagi-Uda antenna as a viable and efficient solution within the context of rapidly advancing wireless communication standards.

REFERENCES

[1] M. E. Villapol, W. Liu, J. Gutierrez, J. Qadir, S. Gordon, J. Tan, L. Chiaraviglio, J. Wu and W. Zhang, "A Sustainable Connectivity Model of the Internet Access Technologies in Rural and Low-Income Areas," *ICST Institute for Computer Sciences, Social Informatics and Telecommunications Engineering,* vol. 245, pp. 93-102, 2018.

[2] F. Nizam, "4G coverage to be improved, while govt rolls out 5G," New Straits Times, Kuala Lumpur, 2023.

[3] L. Kansal, G. S. Gaba, A. Sharma, G. Dhiman, M. Baz and M. Masud, "Performance Analysis of WOFDM-WiMAX Integrating Diverse Wavelets for 5G Applications," *Wireless Communications and Mobile Computing,* vol. 2021, pp. 1-14, 2021.

[4] P. Kaur, "Yagi-Uda Antenna," 2018.

[5] M. A. Haque, M. Zakariya, S. S. Al-Bawri, Z. Yusoff, M. Islam, D. Saha, W. M. Abdulkawi, M. A. Rahman and L. C. Paul, "Quasi-Yagi antenna design for

LTE applications and prediction of gain and directivity using machine learning approaches," *Alexandria Engineering Journal,* vol. 80, pp. 383-396, 2023.

[6]   M. A. Ashraf, K. Jamil, A. Telba, M. A. Alzabidi and A. R. Sebak, "Design and Development of a Wideband Planar Yagi Antenna Using Tightly Coupled Directive Element," *Micromachines (Basel),* vol. 11, no. 11, p. 975, 2020.

[7]   B. Subba, T. Tenzin, S. Norbu, T. Tobgay and T. Zangmo, "Tuning of Yagi Uda Antenna with Gain Enhancement at 300 Mhz and 2.4 Ghz Bands For Wi-Fi Application," *International Journal of Innovative Technology and Exploring Engineering (IJITEE),* vol. 8, no. 9, pp. 2278-3075, 2019.

[8]   Y. Ye, X. Zhao and J. Wang, "Compact High-Isolated MIMO Antenna Module With Chip Capacitive Decoupler for 5G Mobile Terminals," *IEEE Antennas and Wireless Propagation Letters,* vol. 21, no. 5, pp. 928-932, 2022.

[9]   M. Y. Zvezdina, Y. A. Shokova, O. Y. Nazarova, H. T. A. Al-Ali1 and G. H. A. Al-Farhan, "Visualization of electromagnetic exposure near LTE antennae," in *IOP Conference Series: Earth and Environmental Science, Volume 115, All-Russian research-to-practice conference "Ecology and safety in the technosphere" 6–7 March 2017, Yurga, Russian Federation*, Russia, 2018.

[10] N. S. Razak and S. M. Shah, "Antenna for 5G Mobile Communication at 28 GHz," *JOURNAL OF ELECTRONIC VOLTAGE AND APPLICATION,* vol. 3, no. 1, pp. 33-44, 2022.

[11] M. A. Haque, M. A. Zakariya, N. S. S. Singh, M. A. Rahman and L. C. Paul, "Parametric study of a dual-band quasi-Yagi antenna for LTE application," *Bulletin of Electrical Engineering and Informatics,* vol. 12, no. 3, pp. 1513-1522, 2023.

[12] S. Broto and R. Mahardika, "Yagi Biquad Antenna Design for 4G LTE in 2100-2400MHz Frequency Band," in *Proceedings of the 1st Workshop on Mutidisciplinary and Its Applications Part1, WMA-01*, Aceh, Indonesia, 2019.

[13] G. Harridoss, S. Ravimaran, J. William, M. Wasim and M. Abdulah, "High Gain Series Fed Two Dipole Array Antenna with Reduced Size for LTE Application," *IETE Journal of Research,* vol. 68, no. 2, pp. 1080-1090, 2020.

[14] A. Ullah, N. O. Parchin, A. S. I. Amar and R. A. Abd-Alhameed, "Eight-Element Antenna Array with Improved Radiation Performances for 5G Hand-Portable Devices," *Electronics 2022, 11(18),* vol. 2, p. 11, 2022.

[15] S. Kim and J. Choi, "Quasi-Yagi Slotted Array Antenna with Fan-Beam Characteristics for 28 GHz 5G Mobile Terminals," *Applied Sciences,* vol. 10, no. 21, pp. 7686-7686, 2020.

[16] K. M. Morshed, D. K. Karmokar and K. P. Esselle, "Antennas for Licensed Shared Access in 5G Communications with LTE Mid- and High-Band Coverage," *Sensors,* vol. 23, no. 4, pp. 2095-2095, 2023.

[17] M. H. Shamsusudin, I. M. Ibrahim and K. Ulagan, "4G LTE Directional Antenna Design at 1.8 GHz Frequency," in *Proceedings of 4th International Conference on Telecommunication, Electronic and Computer Engineering*, Manila, Philippines, 2022.

[18] M. H. Shamsudin, I. M. Ibrahim, A. J. A. Al-Gburi and T. Purnamirza, "Influence analysis of director's elements on the circular Yagi disc antenna performance at 1.8 GHz," *International Journal of Electrical and Computer Engineering (IJECE),* vol. 13, pp. 6426-6434, 2023.

[19] Al-Gburi and A. J. Abdullah, "Wideband Microstrip Patch Antenna for Sub 6 GHz and 5G Applications," in *PRZEGLĄD ELEKTROTECHNICZNY*, 2021.

[20] B. Bonev, Z. Radkova, L. Dimcheva and P. Petkov, "Minkowski Fractal Yagi Antenna," in *ICEST 2018*, Sozopol, Bulgaria, 2018.

[21] O. S. Baskoro, P. K. S. I Putu Ardana and A. Munir, "A 2x2 Inset Feed Circular patch Antenna Array for 1.8GHz LTE Application," in *2018 4th International Conference on Wireless and Telematics (ICWT)*, 2018.

[22] A. R. Dewan, A. Ibrahim, R. Dewan, A. R. Razali and A. A. Bakar, "Multiband Microstrip Patch Antenna for LTE Application," *International Journal of Nanoelectronics and Materials,* vol. 14, no. 2, pp. 169-178, 2021.

[23] N. O. Parchin1, H. J. Basherlou, Y. I. A. Al-Yasir, A. M. Abdulkhaleq, R. A. Abd-Alhameed and a. P. Excell, "Eight-Port MIMO Antenna System for 2.6 GHz LTE Cellular Communications," *Progress In Electromagnetics Research C,* vol. 99, pp. 45-59, 2020.

[24] S. U. Anuar, M. H. Jamaluddin, J. Din, K. Kamarudin, M. H. Dahri and I. H. Idris, "Triple band MIMO dielectric resonator antenna for LTE applications," *AEU-International Journal of Electronics and Communications,* vol. 118, pp. 153172-153172, 2020.

[25] Abed, A. Tawfeeq, A. Mahmood and Jawad, "Compact Size MIMO Amer Fractal Slot Antenna for 3G, LTE (4G), WLAN, WiMAX, ISM and 5G Communications," *IEEE Access,* vol. 7, pp. 125542-125551, 2019.

[26] M. K. Mohsen, M. Isa, T. Rahman, M. K. Abdulhameed, A.A.M.Isa, M.S.I.M.Zin, S.Saat, Z.Zakaria, I.M.Ibrahim, M.Abu and A.Ahmad, "Novel Design and Implementation of MIMO Antenna for LTE Application," *Journal*

of Telecommunication, Electronic and Computer Engineering, vol. 10, no. 2-8, pp. 2289-8131, 2018.

[27] A. H. Ilyasaha, M. R. Hidayat and S. U. Prini, "2x1 Truncated Corner Microstrip Array Antenna to Increase Gain and Bandwidth for LTE Applications at 2.3 GHz Frequency," *Jurnal Elektronika dan Telekomunikasi (JET),* vol. 22, no. 1, pp. 14-22, 2022.

[28] I. S. Ammer, M. S. Alsahulli and A. A. A. Agnya, "Performance Optimization of Microstrip Patch Antenna Array for WLAN and LTE 4G Technologies.," *JEEEIT TRANSACTIONS,* vol. 1, no. 1, pp. 30-34, 2020.

[29] Dassault Systemes, "CST Studio Suite," Dassault Systemes, 2002-2024. [Online]. Available: https://www.3ds.com/products/simulia/cst-studio-suite. [Accessed 24 November 2023].

[30] K. Street, "Antenna Specification," Chelton, 2023. [Online]. Available: https://www.european-antennas.co.uk/antenna-types-theory/antenna-specification/#:~:text=Most%20antennas%20are%20designed%20to,between%209.5%20to%2010.5GHz.. [Accessed 21 May 2023].

[31] Huawei Consumer, "B310s LTE CPE Quick Start," [Online]. Available: https://www.192-168-1-1-ip.co/manuals/8697.pdf. [Accessed May 2023].

[32] L. Huawei Technologies Co, "Product Description, "Huawei B315s-22 LTE CPE"," L. Huawei Technologies Co, 2014.

[33] Saoudi and B. Hadi, "Analysis and Study the Performance of Coaxial Cable Passed On Different," *Dielectrics,* vol. 13, no. 3, pp. 1664-1669, 2018.

[34] B. Bacha, V. Samlyuk and A. Blednykh, "Measurement of beam-induced power in the NSLS-II diagnostic stripline," *US Department of Energy Office of Scientific and Technical Informtion,* 2019.

[35] K. Le, J. Gilbrech, M. Joyce, J. sanchez-Roddy, Tyler, Talbot, S. Heidger and J. Schrock, "High Voltage Coaxial Cable Pulse Capabilities," in *2023 OEEE Pulsed Power Conference (PPC)*, San Antonio, TX, USA, 2023.

[36] A. Ahmed, "Understanding and Design of Yagi-Uda Antenna," 2022.

[37] Malaysia Communications and Multimedia Commission (MCMC), "Spectrum Assignments for 2600MHz Band," Malaysia Communications and Multimedia Commission (MCMC) | Suruhanjaya Komunikasi dan Multimedia Malaysia (SKMM), Malaysia, 2022.

[38] Malaysia Communication and Multimedia Commissions (MCMC), "Allocation of spectrum bands for mobile broadband service in Malaysia," Malaysian Communications and Multimedia Commission (MCMC) | Suruhanjaya Komunikasi dan Multimedia Malaysia (SKMM), 2019.

[39] G. M. Putra, E. Budiman, Y. Malewa, D. Chyadi, M. Taruk and U. Hairah, "4G LTE Experience: Reference Signal Received Power, Noise Ratio and Quality," in *2021 3rd East Indonesia Conference on Computer and Information Technology (EIConCIT)*, Surabaya, Indonesia, 2021.

[40] S. Pramono, L. Alvionita, M. D. Ariyanto and M. E. Sulistyo, "Optimization of 4G LTE (Long Term Evolution) Network Coverage Area in Sub Urban," in *AIP Conference Proceedings 2217, 030193 (2020)*, Surakarta, Indonesia, 2020.

[41] United Nations, "Goal 4 | Department of Economics and Social Affairs," United Nations, 2022. [Online]. Available: https://sdgs.un.org/goals/goal4. [Accessed 5 January 2024].

[42] United Nations, "Goal 4 Targets," United Nations, 2023. [Online]. Available: https://malaysia.un.org/en/sdgs/12. [Accessed 11 1 2023].

[43] United Nations, "Goal 12 | Department of Economics and Social Affairs," 2023. [Online]. Available: https://sdgs.un.org/goals/goal12. [Accessed 5 January 2024].

[44] S. a. B. D. United Nations in Malaysia, "Goal 12 Targets," United Nations, 2023. [Online]. Available: https://malaysia.un.org/en/sdgs/4. [Accessed 11 1 2023].

APPENDICES

Appendix A: Yagi Antenna Specifications
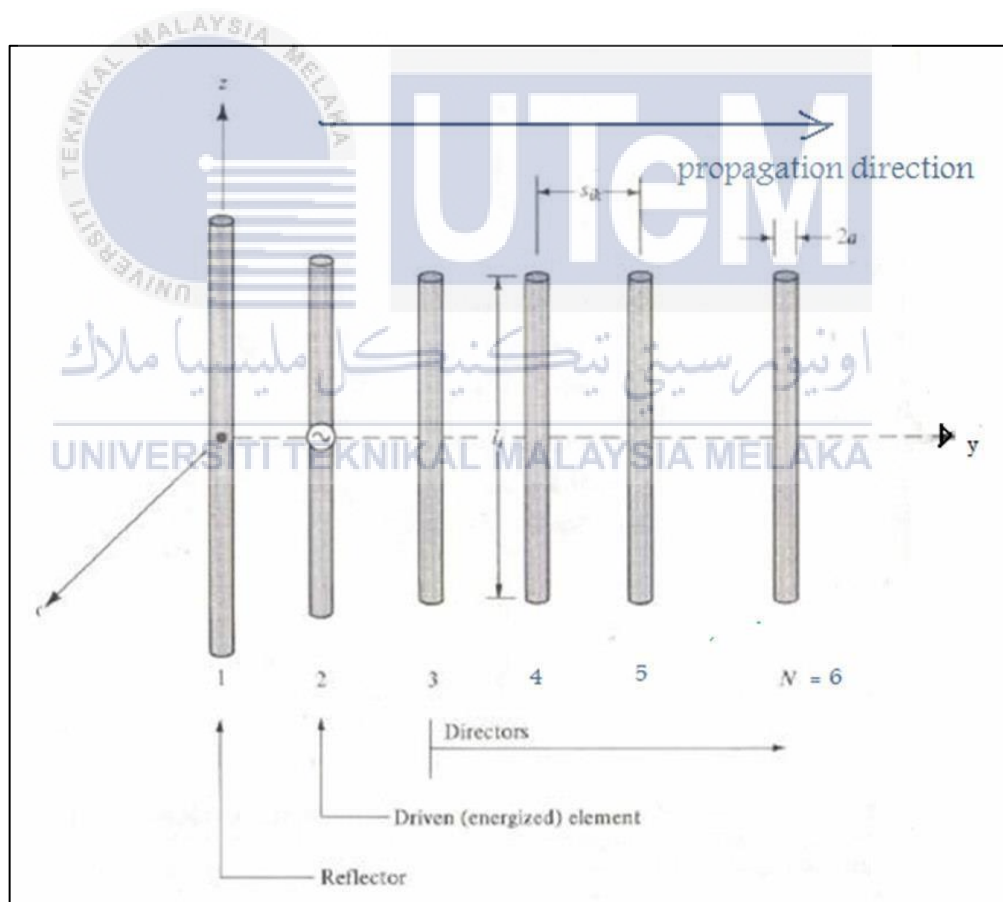
Appendix B: Comparison of Huawei LTE CPE B315 and Huawei LTE CPE B310

Model	Huawei LTE CPE B315	Huawei LTE CPE B310
Product type	LTE Wi-Fi router	LTE Wi-Fi router
Category	LTE Cat.4	LTE Cat.4
Chipset	Hisilicon Balong	Hisilicon Balong
Data rates	DL 150Mbps/UL 50Mbps	DL 150Mbps/UL 50Mbps
Supported 4G LTE frequency bands	• **Huawei B315s-22**: B1/B3/B7/B8/B20/B38 • **Huawei B315s-607**: Band 1/3/7/8/28/40 • **Huawei B315s-936**: Band 1/3/40/41 • **Huawei B315s-608**: Band 1/3/5/7/28	• **Huawei B310s-927**: B1/B3/B8/B40 • **Huawei B310As-852**: B3/B7/B8/B38/B39/B40/B41 • **Huawei B310s-22**: B1/B3/B7/B8/B20 • **Huawei B310s-518**: B1/B2/B4/B5/B7/B28
WLAN	802.11b/g/n, 2.4GHz	802.11b/g/n, 2.4GHz
Max supported users	32 users	32 users
Connector for external antenna	Two, SMA-female jacks	Two, SMA-female jacks
Dimensions	186.0mm x 139.0mm x 46.0mm	181.0mm x 126.0mm x 70.0mm

| Other Features	VoIP, DHCP, NAT, IPv6/IPv4 dual stack, Firewall, Port forwarding, DMZ, ALG, Remote management	Voice, DHCP, NAT, ARP, ICMP, DNS Relay, IPv6/IPv4 dual stack, VPN passthrough, Firewall, URL filter, LAN IP filter, DMZ, UPnP, ALG, Port forwarding
Price	RM225	RM195

Appendix C: Coaxial Cable Comparison

| Type	RG6	LMR240
Impedance	75 Ω	50 Ω
Core thickness (mm)	0.74 mm	1.42mm
Dielectric	PE	Foam PE
Outside Diameter	8.4mm	6.10mm
Shield	-Silver plated copper braid -Copper braid	-Aluminum tape -Tinned copper braid
Maximum attenuation	11dB/100 ft (1000 MHz)	20.4 dB/100ft (5800MHz)
Price/10m	RM19	RM39

Notes: Data from datasheet by PASTERNACK, The engineer's RF source

Appendix D: Antenna settings in Huawei IP address
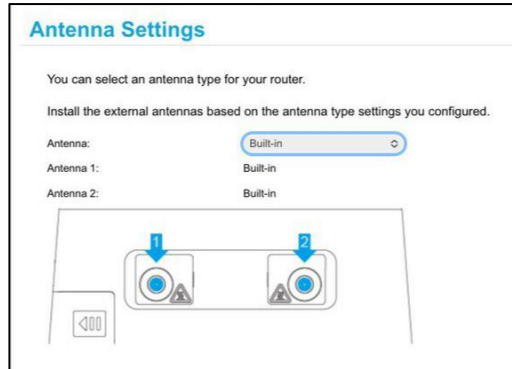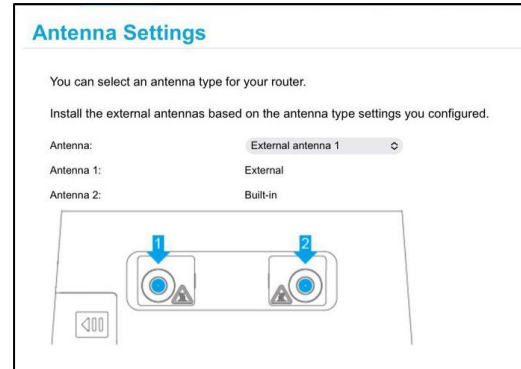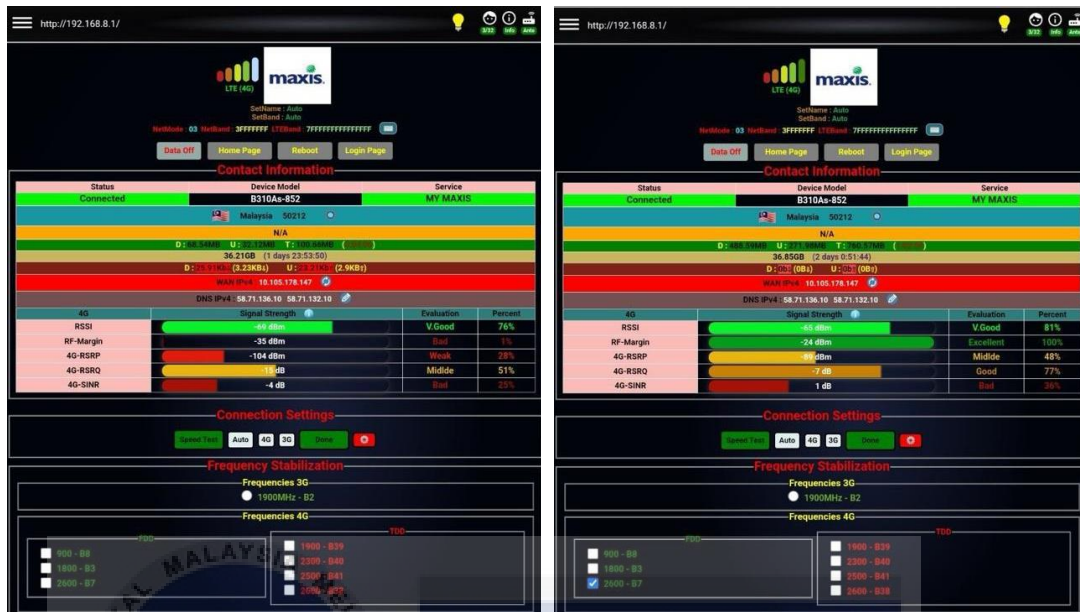

| (a) Built-in Antenna | (b) External Antenna |

Appendix E: Signal Strength Measurement using Huawei Manager Application

(a) Using built-in antenna   (b) Using proposed antenna

Appendix F: Speed-Test Before and After Using Proposed Antenna

    (a) Before using proposed antenna   (b) After using proposed antenna

Appendix G: RSRP, RSRQ, SINR Indicator Standard

RSRP

Range (dBm)	Category
-80 to -44	Excellent
-90 to -80	Good
-100 to -90	Fair
-110 to -100	Poor
-140 to -110	Very Poor

RSRQ

Range (dBm)	Category
-10 to -3	Excellent
-12 to -10	Good
-14 to -12	Fair
-17 to -14	Poor
-20 to -17	Very Poor

SINR

Range (dBm)	Category
10 to 30	Excellent
3 to 10	Good
0 to -3	Fair
-20 to -3	Poor